NASA TECHNICAL NOTE

NASA TN D-5315

NASA TN D-5315

c. 1

AN EXPERIMENTAL INVESTIGATION OF THE MIXING OF COMPRESSIBLE-AIR JETS IN A COAXIAL CONFIGURATION

by James M. Eggers and Marvin G. Torrence

Langley Research Center
Langley Station, Hampton, Va.

NATIONAL AERONAUTICS AND SPACE ADMINISTRATION • WASHINGTON, D. C. • JULY 1969

1. Report No. NASA TN D-5315	2. Government Accession No.	3. Recipient's Catalog No.
4. Title and Subtitle AN EXPERIMENTAL INVESTIGATION OF THE MIXING OF COMPRESSIBLE-AIR JETS IN A COAXIAL CONFIGURATION		5. Report Date July 1969 6. Performing Organization Code
7. Author(s) James M. Eggers and Marvin G. Torrence		8. Performing Organization Report No. L-5632
9. Performing Organization Name and Address NASA Langley Research Center Langley Station Hampton, Va. 23365		10. Work Unit No. 722-03-00-04-23 11. Contract or Grant No.
12. Sponsoring Agency Name and Address National Aeronautics and Space Administration Washington, D.C. 20546		13. Type of Report and Period Covered Technical Note 14. Sponsoring Agency Code

15. Supplementary Notes

16. Abstract

An experimental investigation has been made to obtain data on the mixing of parallel, circular, compressible-air jets in a coaxial configuration. A Mach 1.3 outer jet and a near-sonic central jet, both exhausting to a quiescent atmosphere, were studied. Data were also obtained with both jets operating at subsonic Mach numbers. Radial distributions of total pressure, static pressure, and mass-fraction concentration (air in air) of the central-jet gas were determined at downstream axial stations both in the near-jet and far-jet flow fields. Concentration measurements were made by using a tracer-gas technique. The central-jet gas was a 1-percent mixture of ethylene in air. At each test condition, the total temperature of both jets was approximately 300^0 K (80^0 F). The Reynolds numbers for the supersonic and subsonic outer-jet flow were approximately 42.1×10^6 and 13.9×10^6 per meter (12.8×10^6 and 4.24×10^6 per foot), respectively. Results of the investigation indicate that good correlation with the experimental air mixing data can be obtained by using an eddy viscosity model based on a representative width of the mixing zone and on the center-line mass flow per unit area. The concentration decay in the region well downstream of the concentration potential core was found to be inversely proportional to the square of the axial coordinate. The accuracy of the concentration measurements was found to be significantly affected by sampling technique and sampling-probe design.

17. Key Words Suggested by Author(s) Fluid mechanics Turbulent mixing	18. Distribution Statement Unclassified – Unlimited

19. Security Classif. (of this report) Unclassified	20. Security Classif. (of this page) Unclassified	21. No. of Pages 51	22. Price* $3.00

*For sale by the Clearinghouse for Federal Scientific and Technical Information
Springfield, Virginia 22151

AN EXPERIMENTAL INVESTIGATION OF THE MIXING OF COMPRESSIBLE-AIR JETS IN A COAXIAL CONFIGURATION

By James M. Eggers and Marvin G. Torrence
Langley Research Center

SUMMARY

An experimental investigation has been made to obtain data on the mixing of parallel, circular, compressible-air jets in a coaxial configuration. A Mach 1.3 outer jet and a near-sonic central jet, both exhausting to a quiescent atmosphere, were studied. Data were also obtained with both jets operating at subsonic Mach numbers. Radial distributions of total pressure, static pressure, and mass-fraction concentration (air in air) of the central-jet gas were determined at downstream axial stations both in the near-jet and far-jet flow fields. Concentration measurements were made by using a tracer-gas technique. The central-jet gas was a 1-percent mixture of ethylene in air. At each test condition, the total temperature of both jets was approximately 300° K (80° F). The Reynolds numbers for the supersonic and subsonic outer-jet flow were approximately 42.1×10^6 and 13.9×10^6 per meter (12.8×10^6 and 4.24×10^6 per foot), respectively.

Results of the investigation indicate that good correlation with the experimental air mixing data can be obtained by using an eddy viscosity model based on a representative width of the mixing zone and on the center-line mass flow per unit area. The concentration decay in the region well downstream of the concentration potential core was found to be inversely proportional to the square of the axial coordinate. The accuracy of the concentration measurements was found to be significantly affected by sampling technique and sampling-probe design.

INTRODUCTION

An important application of the turbulent mixing of compressible parallel jets is in the design of hypersonic ramjet-engine combustors. Although injection of the fuel perpendicular to the airstream offers the advantage of greater penetration, the downstream momentum of parallel-injected fuel can contribute significantly to the engine thrust. (See ref. 1.) Since both the fuel distribution and combustor length will have an effect on the ramjet-engine performance, development of analytical techniques to predict the combustor

flow field in order to optimize the combustor design is desirable. Current analytical techniques employ eddy viscosity formulations derived from nonreacting flow data, since extensive measurements representative of the severe environment of the ramjet combustor are not available. The assumption is made in the analysis that the mixing of the reacting flow field is adequately expressed by the parameters (for example, velocity, density, and mixing-zone width) in the nonreacting-flow eddy viscosity formulation.

An analysis of the mixing of the turbulent flow fields has recently been performed by employing the laminar-flow boundary-layer equations modified by replacing the laminar viscosity with the eddy viscosity and by replacing the laminar Prandtl, Lewis, and Schmidt numbers by their turbulent counterparts. In reality, the eddy viscosity is a complex function of the local properties in the flow field, but an assumption of uniform eddy viscosity across the mixing zone is usually applied to facilitate computations. Since the introduction of Prandtl's mixing length theory in 1925 and his later simplified eddy viscosity theory in 1942, which was based on the difference in velocity across the mixing zone (see ref. 2), many eddy viscosity formulations have been proposed (see refs. 3, 4, 5, 6, 7, and 8). No universally accepted eddy viscosity expression is currently available. Recent attempts have been made to gain sufficient knowledge of the eddy viscosity distribution to develop improved eddy viscosity models and also to determine the associated turbulent Prandtl, Lewis, and Schmidt numbers by calculating these parameters directly from experimental data. (See refs. 1, 9, 10, and 11.) Extreme difficulties, however, arise in determining these parameters by this direct method, since derivatives must be obtained from the experimental data. The result is a significant scatter of the values obtained; thus this method was not used herein.

The current experimental investigation was designed to supply data to aid in developing a turbulent mixing analysis and the associated eddy viscosity formulation. Compressible, turbulent mixing data were obtained from coaxial, parallel air jets which exhausted to a quiescent atmosphere. A Mach 1.3 outer jet, approximately 17.8 cm (7.0 in.) in diameter, surrounded a near-sonic central jet with a 2.443-cm (0.962-in.) diameter. In a later stage of the experiment, this central jet was replaced by a smaller 1.036-cm-diameter (0.408-in.) central jet to permit data acquisition at far downstream locations in terms of central-jet diameter in the flow field. Data were also obtained with the smaller central jet exhausting at Mach 0.47 and the outer jet at Mach 0.58. In all tests, the total temperature of the central and outer jet was approximately 300° K (80° F). The Reynolds numbers for the supersonic and subsonic outer-jet flow were approximately 42.1×10^6 and 13.9×10^6 per meter (12.8×10^6 and 4.24×10^6 per foot), respectively. Radial distributions of total pressure, static pressure, and concentration of the central-jet gas (the latter by the tracer-gas technique) were obtained at various locations both in the near-jet and far-jet flow fields.

Data correlation was performed by employing the analysis of reference 7 in conjunction with an improved eddy viscosity model. This analysis was selected to correlate the data because of its immediate applicability to combustion problems. A discussion of the inaccuracies of gas samples taken from flowing streams is presented in the appendix.

SYMBOLS

The units used for the physical quantities defined in this paper are given both in the International System of Units (SI) and in the U.S. Customary Units. Factors relating the two systems are given in reference 12.

A	area
b	a mixing-zone width defined as the radial distance between the points where the velocities are u_1 and u_2
D	central-jet inside diameter (see fig. 1)
I	the ratio of integrated central-jet flow rate calculated by using the measured pressures, temperatures, and mass concentrations, the latter obtained by use of the high-flow-rate sampling system, to the metered central-jet flow rate
I'	the ratio of integrated central-jet flow rate calculated by using the measured pressures, temperatures, and mass concentrations, the latter obtained by use of the low-flow-rate sampling system, to the metered central-jet flow rate
k	empirical constant employed in eddy viscosity formulations
M	Mach number
$\dot{m}$	local mass flow rate
$\dot{m}_c$	jet flow rate calculated by using equation (1)
N_{Le}	turbulent Lewis number, the product of the turbulent diffusion coefficient and the constant-pressure specific heat divided by the turbulent thermal-conductivity coefficient

N_{Pr}	turbulent Prandtl number, the product of the constant-pressure specific heat and the turbulent viscosity divided by the turbulent thermal-conductivity coefficient
N_{Sc}	turbulent Schmidt number, the ratio of the turbulent Prandtl number to the turbulent Lewis number
p	static pressure
T_t	total temperature
u	velocity
u_1	velocity defined by equation (5)
u_2	velocity defined by equation (6)
u_x	free-stream velocity modified for static-pressure changes at the x location (see eq. (3))
V	local velocity modified for static pressure and free-stream velocity deviations (see eq. (3))
V_p	velocity modified for static-pressure changes (see eq. (3))
x	axial coordinate (see fig. 4)
x_l	potential core length based on concentration
y	radial coordinate (see fig. 4)
z	a mixing-zone width based on the distance from the jet center line to the point where the velocity is the mean velocity in the mixing zone
α	local mass concentration obtained by using the high-flow-rate sampling system
α'	local mass concentration obtained by using the low-flow-rate sampling system

ϵ_t eddy viscosity

$\epsilon_{t,o}$ eddy viscosity evaluated at the jet exit station

ρ density

Subscripts:

a evaluated in the quiescent atmosphere

CL evaluated on the jet center line

e evaluated in the outer-jet flow in the region of uniform velocity at the jet exit station

j evaluated at the central-jet exit station and on the center line

max maximum

∞ evaluated in the outer-jet flow external to the mixing zone in the region of uniform velocity

APPARATUS

Nozzle

A sketch of the nozzle section is shown in figure 1. The nozzle contour was designed by using a modification of the technique of reference 13. Reference 13 derives analytical expressions for the design of axisymmetric Laval nozzles and expresses the desired contour as a function of the radial and axial coordinates. The analytical expressions of reference 13 were modified to predict the area ratio as a function of axial distance for the desired Mach 1.3 plug nozzle. This design technique gave a reproducible method of generating a contour and resulted in a nozzle which produced an acceptable exit-velocity profile. However, significant shock waves are evident in the schlieren photographs of figure 2. Pressure measurements indicated the central-nozzle lip shock corresponded to about a 2.5° turning of the outer-jet flow, or approximately a 6-percent change in velocity of the outer jet. Similarly, the outer-nozzle lip shock was found to correspond to about a 1.5° to 2° turning of the outer-jet flow. The outer-nozzle lip shock caused difficulties in data reduction as it impinged upon the central-nozzle flow and imposed a pressure rise upon the center region of the jet flow field. Further discussion of the effects of the shocks will be found in the section entitled "Presentation of Data."

Test Procedure

The nozzle section of figure 1 was connected to a blower system with sufficient capacity to permit continuous operation of the nozzles. The nozzle exhaust pitot pressures were computed from the design exit Mach numbers by assuming that the exit static pressure was atmospheric. Reference pressures were monitored on mercury manometers to insure that the computed pitot pressures were maintained. Ethylene-tracer flow was metered by a variable-area orifice meter and injected into the central-jet air flow far upstream of the nozzle section to insure uniform concentration at the nozzle exit. The ethylene-tracer flow rate was approximately 1 percent by mass of the central-jet air-flow rate.

After steady-state conditions were attained, point by point traverses of the flow field with a rake containing a pitot probe and static-pressure probe (one probe trailed the other along the line of the traverse) were made throughout the unconfined flow field. Pertinent information on the rake and probes is shown in figure 3. A flow-field schematic with the nomenclature used is shown in figure 4. A single-pass schlieren system was used to visually observe and photographically record the jet flow fields. Other supporting measurements recorded include probe location, total temperature of both jets, static pressure from the taps around the inside of the outer-nozzle lip (see fig. 1), barometric readings, and central-jet flow rate. The central-jet air flow was measured by a calibrated thin-plate-orifice meter.

Gas samples were extracted from the flow field through the pitot probe by using only the pitot pressure as the pumping force. Approximately 3 percent of the sample flow was routed through a gas chromatograph and analyzed for ethylene content. The remainder of the sample flow was bypassed and discharged to the atmosphere. (Further details on sampling technique are discussed in the appendix.) Both the flow through the gas chromatograph and the bypass flow were measured by flow meters. Data-acquisition time was approximately 3 minutes per data point and was essentially fixed by the time of the gas-chromatograph-analysis cycle. A discussion of concentration measurement technique and theory by use of the gas chromatograph may be found in reference 14. Data were obtained for the three test conditions shown in the following table:

Test condition	Central-jet diameter	M_j	M_e	$\frac{u_j}{u_e}$	$\frac{T_{t,j}}{T_{t,e}}$	$\left(\frac{x}{D}\right)_{max}$
1	2.443 cm (0.962 in.)	0.942	1.302	0.736	1.0	49
2	1.036 cm (.408 in.)	.813	1.268	.648	1.0	114
3	1.036 cm (.408 in.)	.47	.58	.827	1.0	85

Several samples of the central-jet gas were extracted from the piping upstream of the nozzle exit at the beginning and end of each test. The chromatograph output from the analysis of these samples was set to correspond to full-scale pen deflection on a recorder. This procedure established a central-jet reference concentration based on ethylene which corresponded to 100 percent mass concentration of central-jet gas. (Although the gas chromatograph analysis yields mole concentration, for gases of nearly equal molecular weights as between ethylene and air, mole and mass concentration are equivalent.) The chromatograph output was experimentally verified to be linear with concentration. Therefore, a sample which produced a 50 percent full-scale pen deflection from the chromatograph output contained 50 percent as much ethylene as the central-jet gas, and thus the mass concentration of the sample was 50 percent of that of the central-jet gas. The reduced-concentration data are reported in terms of local mass fraction α of central-jet gas. For clarity, the units of α may be thought of as the ratio of pounds central-jet gas per pound of mixture.

Accuracy of Results

Based on the chart resolution of the recorded pitot pressures and an uncertainty of the total-temperature measurement of $\pm 6^{\circ}$ K ($\pm 10.8^{\circ}$ F), it is estimated that the velocity data are accurate to ± 2 percent. This accuracy does not include any uncertainty due to the static pressure measurements. In the data of test conditions 1 and 2, the static pressure was not uniform in either the axial or radial direction.

One means of assessing the accuracy of the data is to apply the principle of conservation of mass to the central-jet flow. The following equation is evaluated for each axial station at which data are obtained for this assessment:

$$\dot{m}_c = \int_A \alpha(\dot{m}/A)dA \tag{1}$$

where $\dot{m}/A$ is the local mass flow per unit area evaluated from the total temperature, pitot pressure, and static pressures measured, α is the local mass concentration, and A is the area of the flow field over which α is nonzero. If the data are correct, $\dot{m}_c$ will be equal to the central-jet flow rate. Differences between $\dot{m}_c$ and the experimentally determined central-jet flow rate obviously are due to experimental error. A comparison between these two mass-flow quantities is an essential criterion in assessing the accuracy of concentration measurements because of uncertainties in obtaining representative samples from flowing streams.

The application of equation (1) to the data presented herein is reported in the appendix. Large errors in concentration measurements taken from binary streams may occur,

the probe design and sampling technique employed having a significant effect upon the results. The actual physical mechanism which causes unrepresentative sample collection is not known, but satisfactory measurements were obtained with the probe and sampling technique used in this investigation. The results suggest that the erroneous concentration measurements are related to the local turbulence level in the flow field.

Theory

The analysis of reference 7 employs equilibrium chemistry, transformation, and explicit finite difference techniques to compute turbulent mixing and combustion of parallel unconfined streams of hydrogen and air. Both two-dimensional and axisymmetric configurations are treated, the method differing only slightly in the transformation employed. The analysis has provision for axial pressure gradients and nonunity turbulent Prandtl and Lewis numbers. Principal inputs to the mixing program are distributions of velocity, static temperature, and mass concentration corresponding to equal increments of the stream function. This input requirement is inconvenient for other than step profiles as considerable calculation is required to determine the stream-function distribution. The analysis initially contained an eddy viscosity formulation attributed by reference 15 to Zakkay. The Zakkay formulation was based on experimental concentration data obtained downstream of the potential core and was intended to be used only in far-field calculations. It was emphasized that the Zakkay eddy viscosity formulation predicts a concentration decay proportional to $1/x^2$. Zakkay's eddy viscosity formulation has the form:

$$\epsilon_t = kz(\rho u)_{CL} \tag{2}$$

In equation (2), ϵ_t is the eddy viscosity, z is the mixing-zone width based on the distance from the jet center line to the point where the velocity is the mean velocity in the mixing zone, ρ is the density, and u is the velocity. A value of 0.04 for the empirical constant k was suggested in reference 7 to be used in conjunction with turbulent Prandtl and Lewis numbers of unity, step velocity-profile input, and mixing of hydrogen and air. More detailed information on the mixing program is contained in references 7 and 15.

In order to analyze the air-in-air mixing data obtained herein, the central jet was input as standard air and the outer jet was input as 100 percent nitrogen. The oxygen concentration could be interpreted as a tracer gas in the same manner that ethylene was used in obtaining the experimental data.

PRESENTATION OF DATA

The experimental data of test conditions 1 and 2 are presented in figures 5 and 6, respectively. It was observed during reduction of the data for test conditions 1 and 2 that

the experimental static-pressure distributions were not uniform in either the axial or radial direction. A nonuniform, radial static-pressure distribution is not provided for in current mixing analyses; therefore, it was necessary to devise a data-reduction method whereby the nonuniformity of static pressure could be eliminated from the data.

Two possible methods to reduce the data were suggested. The first method was to assume uniform static pressure equal to atmospheric pressure throughout the flow field. The second method was to use the static-pressure distribution from the nozzle exit to reduce the data at the downstream stations. The second method was chosen because retention of a true representation of the initial mixing conditions was desirable and an assumption of uniform static pressure was unrealistic. Center-line static-pressure ratios, that is, measured static pressure divided by atmospheric pressure, for test condition 1 are tabulated as follows:

x/D	0	11.0	17.2	25.0	30.0	36.0	49.0
p/p_a	1.11	1.18	1.15	1.15	1.15	1.11	1.04

The static pressure at all axial locations except the jet exit generally decreased with increasing radial dimension until ambient-pressure levels were attained.

The outer-jet-exit static pressure was determined from the static taps around the outer-nozzle exit and from the probe static-pressure measurement. Where shock waves did not intercept the static-pressure probe, the probe and static-tap measurements were in good agreement. The outer-jet-exit static-pressure ratio p/p_a was 0.98 for test condition 1.

The center-line velocity distribution for test condition 1 obtained by employing the measured static pressure is labeled experiment in figure 5(a). Similar distributions of static pressure were observed in the data of test condition 2. However, even more distinct effects of compressions and expansions were evident and are reflected in the more sizable scatter of the experimental center-line velocity data of figure 6(a). These data were computed by using the measured static pressure. As previously stated, it was desirable to retain the measured nozzle exhaust conditions and reduce all downstream profiles to the static-pressure level at the nozzle exit. As no precise method existed for incorporating this change, because of the radial as well as the axial static-pressure variation, the somewhat arbitrary decision was made to make the static-pressure change along streamlines. Further analyses indicated that for the given conditions the streamlines, actually stream-tube surfaces, were reasonably parallel over the data range. Thus, the data-reduction method allowed static-pressure changes to be made along lines of constant radius. Therefore, in all data except those at the jet exit station, the local measured pitot pressure was used in conjunction with the static pressure measured at the jet exit at the

same radial location to compute local Mach numbers. Velocities were then computed by using an average total temperature of 300° K (80° F) and a specific-heat ratio of 1.4.

In addition to the pressure modification, a second modification was incorporated into the velocity data which compensated for variation of the free-stream velocity. These variations were due to experimental error, to viscous and shock losses and, at the most downstream stations, to penetration of the outer mixing boundaries of the outer jet and surrounding air into the mixing zone (see fig. 4). Similarity of profiles was applied through the following equation:

$$\frac{V - u_j}{u_e - u_j} = \frac{V_p - u_j}{u_x - u_j} \tag{3}$$

where V is the new local velocity modified for pressure and free-stream velocity deviation, u_j is the center-line jet exit velocity, u_e is the velocity evaluated in the outer-jet flow at the jet exit in the region of uniform flow, u_x is the free-stream velocity modified for static-pressure changes at the x location, and V_p is the local velocity modified for static-pressure changes. All velocity data for test conditions 1 and 2, except the basic data points in figures 5(a) and 6(a), have been modified for both static-pressure changes and free-stream velocity deviations according to the previously discussed methods.

The resulting velocity profiles corresponding to test condition 1 are shown in figures 5(c) and 5(d). The magnitude of the free-stream velocity modification is less than 2 percent at x/D less than 30, less than 3 percent at x/D of 30 and 36, and less than 10 percent at x/D of 49. The uncertainty of the overall pressure and velocity modification is reflected in scatter in the velocity data downstream of the inner nozzle lip (for y/D near 0.5) as is evident in the data of figures 5(c) and 5(d).

The resulting velocity profiles corresponding to test condition 2 are shown in figures 6(c), 6(d), 6(e), and 6(f). Pressure and free-stream velocity modifications were made as in the data of test condition 1. For test condition 2 data, the magnitude of the free-stream velocity correction was less than 2 percent at x/D less than 102.8 and less than 4 percent at x/D of 102.8 and 114.2. As in the test condition 1 data, uncertainties of the modifications are evident in the velocity profiles for values of y/D near 0.5.

Concentration distributions for test condition 1 are presented in figures 5(b), 5(e), and 5(f). Concentration distributions for test condition 2 are presented in figures 6(b), 6(g), 6(h), 6(i), and 6(j). The concentration data for both test conditions were consistent except for scatter in the data of test condition 1 at an x/D of 21.4. The four concentration values at an x/D of 21.4 in figure 5(b) represent data obtained from different runs and on different days. No satisfactory explanation for the scatter was found.

Experimental data corresponding to test condition 3 are shown in figure 7. The center-line velocity distribution and the velocity profiles for test condition 3 are shown in figures 7(a) and 7(c) and (d), respectively. No modification for pressure or free-stream velocity variations was applied to the test condition 3 data. Local measurements of pitot and static pressures were used to obtain Mach number distributions. A mean total temperature was then employed to obtain velocity distributions by using a specific-heat ratio of 1.4.

The experimental center-line concentration distribution and the experimental concentration profiles for test condition 3 are shown in figures 7(b) and 7(e) and (f), respectively.

Data Analysis

As previously discussed theoretical analyses of the experimental flow fields were performed by employing the mixing analysis of reference 7 and the associated computer program described in reference 15. As may be seen in figures 5(c), 6(c), and 7(c), the jet exit flow consisted of a large percentage of boundary-layer flow. Therefore, the near-field velocity profiles are not similar, the initial mixing is wakelike in nature, and a step-function velocity-profile input to the mixing program could not be expected to satisfactorily predict the mixing in the near field. Thus, it was necessary to employ a representation of the experimental velocity profiles as inputs to the mixing program. The solid line in figures 5(c), 6(c), and 7(c) at an x/D of zero is representative of the input velocity profiles. Between 23 and 39 input points were employed to represent the profiles, the exact number depending upon the particular test-condition data being analyzed. Since a velocity of zero at the inner-nozzle lip ($y/D = 0.5$) violates the mathematics of the analysis, a low but finite velocity value was used as an input at this location. Step profiles of concentration were employed as inputs for all computations performed, as shown in figures 5(e), 6(g), and 7(e).

Initial computations were performed by using the constants recommended in reference 7, that is, $k = 0.04$, $N_{Pr} = 1.0$, $N_{Le} = 1.0$, and the Zakkay viscosity model (see eq. (2)). The results of these calculations are shown as dashed lines in figures 5(a) and 5(b), 6(a) and 6(b), and 7(a) and 7(b) for test conditions 1, 2, and 3, respectively. It is evident that the Zakkay viscosity model in conjunction with $k = 0.04$, greatly overpredicts the rate of mixing of the air jets for all three test conditions. The theoretical solution for other values of k may be generated from the solution for a given k value by scaling x/D by the ratio of the k's involved. A more nearly correct value of k to be used in conjunction with the Zakkay viscosity model would be on the order of 0.004 for the far-field velocity data. Initial calculations indicated that satisfactory correlation of the near-field mixing data of test condition 1 could be obtained by reducing the constant employed with the Zakkay viscosity model to 0.0025. However, as the Zakkay viscosity model was

formulated for far-field calculations and contains a mixing-zone width which is representative of the mixing zone only in the far field, it is not surprising that continuous calculations throughout the flow field were unsatisfactory. The center-line velocity distribution predicted by the Zakkay viscosity model and by using $k = 0.0025$ is shown in figure 5(a) for the data of test condition 1. It is evident that the Zakkay model does not produce a rapid enough increase in eddy viscosity at the end of the near field to correctly predict the far-field data in one continuous calculation.

Illustrative of the requirement for increasing eddy viscosity at the end of the near field are the preliminary correlations of the test condition 1 data which were presented in reference 16. (The preliminary data of ref. 16 cannot be compared in magnitude with those data presented herein, as a different data-reduction and correlation technique was used.) In reference 16, the Zakkay viscosity model was employed with a k of 0.0025 in the near field ($x/D \leq 16.2$) with a step change of k to 0.006 at the $x/D = 16.2$ location. Thus, the eddy viscosity was increased 2.4 times in the region near the end of the velocity potential core. Good correlation with the experimental data was attained; however, the step change in k with associated discontinuous gradients of concentration and velocity together with the difficulty in determining the proper location in the flow field to make the step change in k made the calculation technique unsatisfactory.

The difficulties in correlating the data by using the step change in k made it evident that a method which would permit continuous calculations throughout the flow field was highly desirable. As a result, the following eddy viscosity expression was formulated:

$$\epsilon_t = kb(\rho u)_{CL} \tag{4}$$

In equation (4), ϵ_t is the eddy viscosity, k is the empirical constant, $(\rho u)_{CL}$ is the mass flow per unit area on the jet center line, and b is the mixing-zone width between the points where the local velocity is u_1 and u_2 as given by equations (5) and (6).

$$u_1 = u_\infty + 0.95(u_{CL} - u_\infty) \tag{5}$$

$$u_2 = u_\infty + 0.50(u_{CL} - u_\infty) \tag{6}$$

The mixing-zone width b thus is based on a width of the mixing zone rather than a distance from the jet center line as in the Zakkay model, and, therefore, has physical significance in both the near-jet and far-jet flow fields.

Calculations for all three test conditions were performed by using the eddy viscosity expression given by equation (4). The resulting theoretical center-line velocity distributions are shown by the solid lines in figures 5(a), 6(a), and 7(a) for test conditions 1, 2, and 3, respectively. Good correlation was obtained for the data of all three test conditions; however, different values of the empirical constant were required for the data of

each test condition. The empirical constants required were 0.0098, 0.0078, and 0.011 for the data of test conditions 1, 2, and 3, respectively. The theoretical velocity profiles are compared with the experimental velocity profiles for test condition 1 in figures 5(c) and 5(d), for test condition 2 in figures 6(c), 6(d), 6(e), and 6(f), and for test condition 3 in figures 7(c) and 7(d). Good agreement between the theoretical velocity profiles and the experimental data is evident in the figures for the data of all three test conditions. Emphasis is placed on the center-line distributions, however, since a reasonable fit throughout the flow field indicates that only one well-selected experimental data point on the center line is necessary to determine the experimental constant k for given initial mixing conditions. It should also be pointed out that the theoretical velocity solutions for all three test conditions are independent of the magnitude of the turbulent Prandtl and turbulent Lewis numbers, as no significant transfer of heat is involved.

The mass concentration of central-jet gas on the center line as predicted by using the analysis of reference 7 and the eddy viscosity model of equation (4) is presented in figures 5(b), 6(b), and 7(b) for test conditions 1, 2, and 3, respectively. Note that solutions for various turbulent Schmidt numbers N_{Sc} (the turbulent Schmidt number is the ratio of the turbulent Prandtl number N_{Pr} to the turbulent Lewis number N_{Le}) are presented, as examples of the effect of the variation of this parameter are quite limited in the literature. It is evident that increasing the Schmidt number by a factor of four (from 0.25 to 1.00) is equivalent to a reduction of the experimental constant by a factor of two to three depending upon its location in the flow field. However, a change in k also would cause a shift in the predicted velocity distribution. Thus, the correlation technique requires, first, employing the experimental center-line velocity distribution to determine the experimental constant k and then employing the center-line concentration distribution to obtain the most appropriate value of turbulent Schmidt number. Whether the turbulent Prandtl number or turbulent Lewis number is 0.60 or 1.00 cannot be determined from the data herein. However, the turbulent Schmidt number is sufficient to determine the uniqueness of the concentration distribution along with the empirical constant k. Inspection of figures 5(b) and 6(b) indicates that reasonable correlation of the center-line concentration distribution is obtained by using a turbulent Schmidt number on the order of 0.60. However, for the test condition 3 data (fig. 7(b)), the turbulent Schmidt number required to correlate the data is somewhat higher. Theoretical calculations for the test condition 3 data were made by using a turbulent Schmidt number of unity. No reason for the differences in the turbulent Schmidt number required for correlation is evident. Inadequacies in the eddy viscosity expression, for example, too fast or too slow mixing at a location in the flow field, will affect not only the velocity but also the predicted concentration distribution. Particularly evident near the end of the concentration potential core is the too rapid mixing of the eddy viscosity model (or possibly the uncertainty in turbulent Schmidt number) which causes underprediction of the center-line concentration.

Theoretical concentration profiles are compared with the experimental data in figures 5(e) and 5(f) for the data of test condition 1, in figures 6(g), 6(h), 6(i), and 6(j) for the data of test condition 2, and in figures 7(e) and 7(f) for the data of test condition 3. Good agreement between theory and the experimental data is evident in the figures for all three sets of experimental data. It is concluded that an eddy viscosity model based on a representative width of the mixing zone and the center-line mass flux per unit area results in good correlation with the air-mixing data reported herein. However, the experimental constant required to correlate the data apparently depends upon the experimental conditions of the data considered.

It has been reported in reference 11 that the decay of center-line mass concentration of axisymmetric jets is inversely proportional to x^2. This decay rate was based on experimental data of jets of various gases, including argon, carbon dioxide, helium, and hydrogen. Figure 8 indicates that the observed concentration decay in the region well downstream of the concentration potential core is approximated by the inverse of the x^2 decay rate. In the data of test conditions 2 and 3, the use of the inverse of the x^2 decay rate to estimate concentration values just downstream of the end of the concentration potential core will result in substantial error for mass concentrations of 50 percent and greater. It was also reported in reference 11 that the concentration potential core length may be computed to a first approximation by the following equation:

$$\frac{x_l}{D} = 11.0\sqrt{\frac{\rho_j u_j}{\rho_e u_e}} \tag{7}$$

(Note the concentration potential core length x_l has been nondimensionalized by the jet diameter here rather than the jet radius as in ref. 11. This changes the value of the constant from 22 to 11 as shown in eq. (7).) This equation was derived by extrapolation of the concentration decay curve ($\alpha \approx 1/x^2$) to 99 percent mass concentration. A comparison of the concentration potential core lengths predicted by equation (7), by the $1/x^2$ extrapolation, and by a smooth extrapolation, the latter of which appears to give the best representation of the data, is shown in the following table:

Test condition	Concentration potential core length, x/D		
	Equation (7)	$1/x^2$ extrapolation	Smooth extrapolation
1	9.4	17.5	13.5
2	8.9	17.0	10.0
3	10.0	14.5	6.0

It is concluded that the concentration potential core length is not accurately predicted by assuming a variation proportional to the square root of the ratio of the central-jet mass

flow per unit area to the outer-jet mass flow per unit area. It is observed that the data from which equation (7) was formulated have a scatter of 30 percent and -50 percent relative to values determined by equation (7), thus accurate predictions could not be expected. Concentration potential core lengths obtained by a smooth extrapolation are shown as dashed lines in figure 8. The experimental center-line jet exit Mach numbers were 0.942, 0.813, and 0.47 for test conditions 1, 2, and 3, respectively. A trend of decreasing concentration potential core length with decreasing central-jet Mach number is noted. This trend is consistent with the smooth extrapolations of figure 8 and with the known fact that lower Mach number streams mix faster and, thus, are expected to have shorter potential core lengths.

Eddy Viscosity Distributions

Since the success of any turbulent mixing analysis depends strongly upon the adequacy of the particular eddy viscosity expression employed, it is instructive to examine the eddy viscosity distribution obtained in the correlation of the turbulent mixing data presented herein. In figure 9, the variation of the ratio of the eddy viscosity at each x/D to the eddy viscosity at the jet exit with x/D is presented. Similar trends of the eddy viscosity increasing at an increasing rate near the jets exit ($x/D < 20$) and of the eddy viscosity varying linearly with x in the far field are evident for the data of all three test conditions. It is apparent in figure 9 that in the far field for a given x/D the curve for test condition 1 is approximately 2.36, the nozzle-diameter ratio, times the curve for test condition 2. (Note that the central-jet mass flow per unit area was approximately equal for the data of test conditions 1 and 2.) Also, for a given x/D the curve for test condition 2 is approximately 1.80, the ratio of mass flows per unit area, times the curve for test condition 3. (Note that the jet diameter was the same for test conditions 2 and 3.) Thus, in the far field, the eddy viscosity scales as $\rho_j u_j D$; however, because the initial velocity profiles are nonsimilar, the near field will not scale in a similar manner. Initial values of the eddy viscosity for the three test conditions are shown in figure 9.

Although the eddy viscosity expression employed correlates the data presented satisfactorily, certain limitations are inherent in the formulation. For example, the mixing-zone width b is based on velocity difference; thus, as the velocity difference between two streams becomes very small, the mixing-zone width becomes indefinite. Furthermore, whether the present eddy viscosity model may be satisfactorily applied to flow fields where large density gradients occur, such as in hydrogen-air mixing, is unknown. Although the empirical constant k required adjusting to correlate the data, it is anticipated that application of this eddy viscosity model to a sufficient quantity of data will produce a relationship which will enable calculation of k for given initial mixing conditions. Since the eddy viscosity is semiempirical in nature, it is too much to expect a single correlation to be valid for all conditions encountered. The eddy viscosity model employed

herein is similar to that employed in reference 17 in which an analysis of the mixing of unconfined jets with quiescent air was performed. In addition the eddy viscosity model used herein was successfully employed in reference 18 to compute two-dimensional mixing of supersonic streams in the presence of shock waves.

CONCLUSIONS

As a result of the experimental and analytical study of the turbulent mixing of circular, coaxial jets the following conclusions were obtained:

1. An eddy viscosity model based on a representative width of the mixing zone and the center-line mass flow per unit area together with the experimentally determined constants resulted in good correlation with the air mixing data reported herein.

2. Large errors in concentration measurements taken from binary streams may occur, the probe design and sampling technique employed having a significant effect upon the results. The actual physical mechanism which causes unrepresentative sample collection is not known, but satisfactory measurements were obtained with the probe and sampling technique used in this investigation. The results suggest that the erroneous concentration measurements are related to the local turbulence level in the flow field.

3. The concentration decay in the region well downstream of the concentration potential core is well approximated by an inverse of the square of the axial coordinate.

4. The concentration potential core length is not accurately predicted by assuming a variation proportional to the square root of the ratio of central-jet to outer-jet mass flow per unit area.

5. Turbulent Schmidt numbers required to correlate the concentration data were found to be approximately 0.6 for the high-velocity data and somewhat larger for the low-velocity data.

Langley Research Center,
National Aeronautics and Space Administration,
Langley Station, Hampton, Va., May 1, 1969,
722-03-00-04-23.

APPENDIX

SAMPLING TECHNIQUE

Large differences in concentration measurements may occur, the sampling technique employed having a significant effect upon the values obtained. In this investigation the central-jet flow computed from the data by using equation (1) was found to be approximately 25-percent less than the metered central-jet flow. In reference 14 similarly evaluated accuracies of ±20 percent were found in mass flows when ethane was used as a tracer gas. In other investigations (refs. 19 and 20), an excess of the larger molecular weight gases were found in the gas samples. Recent literature (ref. 5) stresses the fact that the probe design can radically affect the concentration measurement.

It was postulated that if the probe captured all flow in the stream tube in front of its sampling port, a minimum of sampling bias would occur. Up to this time only sufficient flow to supply the chromatograph (40 cm^3/min) was allowed to pass through the probe and the remaining 97 percent of full stream-tube capture flow was spilled around the probe. The sampling system was modified to remove all possible restrictions from the sampling lines and an internally expanded sampling probe, shown in figure 3, was installed. The modified sampling system passed 40 cm^3/min through the chromatograph and bypassed approximately 1300 cm^3/min during a checkout test. This total probe flow (1340 cm^3/min) accounted for all but about 100 cm^3/min of the computed full-capture probe flow for the checkout condition. New concentration readings were found to be higher than the previously obtained data by approximately the 25 percent required to satisfy continuity of mass of the central-jet flow.

Two sets of concentration data were acquired at test condition 2 by using the pitot probe shown in figure 3. The first set of concentration data was taken with approximately 40 cm^3/min flow through the sampling probe, and the corresponding local mass concentration of central-jet gas will be called α'. The second set of data employed the modified high-flow-rate sampling system discussed previously and the resulting local mass concentration will be called α. Switching from one sampling flow rate to the other was accomplished by opening a bypass valve, thus all other details of the two sampling techniques were identical. The ratio of the integrated to the metered central-jet flow, as determined by using the concentration α', is given the symbol I'. Similarly, the ratio of the integrated to the measured central-jet flow, as determined by using the concentration α, is given the symbol I. Values for these parameters at different values for x/D for the three test conditions are presented in table I. Values for I' are presented only for test condition 2.

APPENDIX

TABLE I.- MASS-FLOW INTEGRATIONS

Test condition 1		Test condition 2			Test condition 3	
x/D	I	x/D	I	I'	x/D	I
0	0.96	0	0.94	---	0	1.02
11.0	1.05	7.34	1.01	0.79	7.34	1.00
17.2	1.04	13.5	1.02	.70	13.5	.96
25.0	.99	20.8	1.03	.53	20.8	.99
30.0	1.05	30.6	1.00	.52	26.2	.95
36.0	1.02	36.7	.99	.45	42.5	1.00
49.0	1.03	44.1	1.05	.44	55.5	1.03
		55.4	.95	.34	73.5	.94
		61.2	.89	.32	85.0	.83
		73.4	.94	.25		
		84.9	.87	.18		
		97.9	.80	.27		
		102.8	.79	---		
		114.2	.88	---		

It is evident from inspecting the values in table I that the low-flow-rate sampling technique accounted for as little as 18 percent of the total central-jet flow at $x/D = 84.9$. The variation of α'/α with local Mach number is shown in figure 10(a). A ratio of α'/α of unity corresponds to no sampling-rate effect, and a value of zero indicates that the high-flow-rate sampling technique detected central-jet gas whereas the low-flow-rate sampling technique found none. The ratio α'/α may also be interpreted as an indication of sampling error by using the low-flow-rate sampling technique. In figure 10(b) the ratio of α'/α is plotted against the radial coordinate to show the location of each point in the flow field. The following observations are made with regard to the data of figures 10(a) and 10(b):

(1) The sampling error is not a function of Mach number alone, as different values of the sampling error α'/α are obtained at identical Mach numbers.

(2) Errors occur in the subsonic flow as well as the supersonic flow. Thus, the explanation of reference 21, in which similar erroneous sampling results are attributed to a detached normal shock, is not applicable here. Similar sampling problems in subsonic flow were found in reference 5.

(3) The sampling error is insensitive to local gradients in the flow field. At the $x/D = 97.90$ station, where the Mach number gradient and the concentration gradient are

small, the ratio α'/α varies from 0.125 to 0.625. Scatter at the far right of figure 10(b) is due to α'/α consisting of the ratio of two experimental quantities which are subject to sizable experimental error as their magnitudes become small.

(4) The few points at x/D of 7.34 and 13.50, which indicate the least sampling-rate effect, are located near the center line of the jets and in the region of the potential core. (See fig. 10(b).) Thus, these points are in a region of relatively low turbulence. The fact that they have very small errors suggests that the sampling errors are related to the local turbulence level in the flow field. A similar effect of no sampling error near the jet exit was found in references 20 and 21. Although the data of reference 21 were generated in a realm of extremely low pressure, the sampling effects are so strikingly similar to those found herein that the same mechanism is suggested.

(5) A separation or pressure diffusion model, similar to those discussed in references 21, 22, and 23, in which light gas molecules are deflected due to streamline curvature near the sampling probe, and heavy gas molecules continue on into the probe, does not appear consistent with the observed fact that no erroneous samples are obtained within the potential core region. In particular, the data of reference 20 also show that in the region of the jet center line, the erroneous sampling results start at approximately the point where the potential core ends.

It is concluded that large errors in concentration measurements taken from binary gas streams may occur and that the sampling technique employed has a significant effect upon the values obtained. It is also concluded that the actual physical mechanism which causes the sampling probe to obtain unrepresentative samples of gaseous mixtures is not known; however, the results suggest that the erroneous concentration measurements are related to the local turbulence level in the flow field.

REFERENCES

1. Morgenthaler, John H.: Supersonic Mixing of Hydrogen and Air. NASA CR-747, 1967.
2. Schlichting, Hermann (J. Kestin, trans.): Boundary Layer Theory. Fourth ed., McGraw-Hill Book Co., Inc., c.1960.
3. Libby, Paul A.: Theoretical Analysis of Turbulent Mixing of Reactive Gases With Application to Supersonic Combustion of Hydrogen. ARS J., vol. 32, no. 3, Mar. 1962, pp. 388-396.
4. Ting, Lu; and Libby, Paul A.: Remarks on the Eddy Viscosity in Compressible Mixing Flows. J. Aero. Sci., vol. 27, no. 10, Oct. 1960, p. 797.
5. Alpinieri, Louis J.: An Experimental Investigation of the Turbulent Mixing of Non-Homogeneous Coaxial Jets. PIBAL Rep. No. 789 (Contract No. AF 49(638)-217), Polytech. Inst. Brooklyn, Aug. 1963.
6. Peters, C. E.: A Model for the Free Turbulent Eddy Viscosity. AEDC-TR-65-209, Nov. 1965.
7. Edelman, R.: Diffusion Controlled Combustion for Scramjet Application. Part I – Analysis & Results of Calculations. Tech. Rep. 569 (Contract No. NAS 1-5117), Gen. Appl. Sci. Lab., Inc., Dec. 1965.
8. Schetz, J. A.: Turbulent Mixing (Analysis). Research and Development Programs. U-RQR/67-1, Appl. Phys, Lab., Johns Hopkins Univ., Jan.-Mar. 1967.
9. Zakkay, Victor; and Krause, Egon: The Radial Variation of the Eddy Viscosity in Compressible Turbulent Jet Flows. ARL 65-89, U.S. Air Force, May 1965. (Available from DDC as AD 617 701.)
10. Eggers, James M.: Velocity Profiles and Eddy Viscosity Distributions Downstream of a Mach 2.22 Nozzle Exhausting to Quiescent Air. NASA TN D-3601, 1966.
11. Zakkay, Victor; Krause, Egon; and Woo, Stephen D. L.: Turbulent Transport Properties for Axisymmetric Heterogeneous Mixing. ARL 64-103, U.S. Air Force, June 1964. (Available from DDC as AD 604 008.)
12. Mechtly, E. A.: The International System of Units – Physical Constants and Conversion Factors. NASA SP-7012, 1964.
13. Foelsch, Kuno: The Analytical Design of an Axially Symmetric Laval Nozzle for a Parallel and Uniform Jet. J. Aeronaut. Sci., vol. 16, no. 3, Mar. 1949, pp. 161-166, 188.
14. Torrence, Marvin G.: Concentration Measurements of an Injected Gas in a Supersonic Stream. NASA TN D-3860, 1967.

15. Hopf, H.; and Fortune, O.: Diffusion Controlled Combustion for Scramjet Applications. Part II – Programmer's Manual. Tech. Rep. 569 (Contract NAS1-5117), Gen. Appl. Lab., Inc., Dec. 1965.

16. Henry, John R.: Fuel Injection and Mixing in Scramjet Combustors. NASA TM X-1437, 1967.

17. Warren, Walter R., Jr.: An Analytical and Experimental Study of Compressible Free Jets. Publ. No.: 23,885, Univ. Microfilms, Inc., 1957.

18. Weidner, John P.; and Trexler, Carl A.: Preliminary Investigation of Momentum Diffusion Between Two Supersonic Airstreams in the Presence of Shock Waves. NASA TN D-4974, 1964.

19. Masson, Bruce S.: Diffusive Separation of a Gas Mixture Approaching a Sampling Probe. Tech. Rep. HE-150-206 (Contract N-onr-222(45)), Inst. Eng. Res., Univ. of California, Oct. 30, 1962.

20. Chow, Reuben R.: On the Separation Phenomenon of Binary Gas Mixture in an Axisymmetric Jet. Rep. No. HE-150-175 (Contract AT(11-1)-34), Inst. Eng. Res., Univ. of California, Nov. 4, 1959.

21. Reis, Victor H.; and Fenn, John B.: Separation of Gas Mixtures in Supersonic Jets. J. Chem. Phys., vol. 39, no. 12, Dec. 15, 1963, pp. 3240-3250.

22. Waterman, P. C.; and Stern, S. Alexander: Separation of Gas Mixtures in a Supersonic Jet. J. Chem. Phys., vol. 31, no. 2, Aug. 1959, pp. 405-419.

23. Becker, E. W.; Beyrich, W.; Bier, K.; Burghoff, H.; and Zigan, F.: The Separation Nozzle II – The Physical Bases and the Expenditures of the Process. AEC-tr-3839, U.S. At. Energy Comm., 1957.

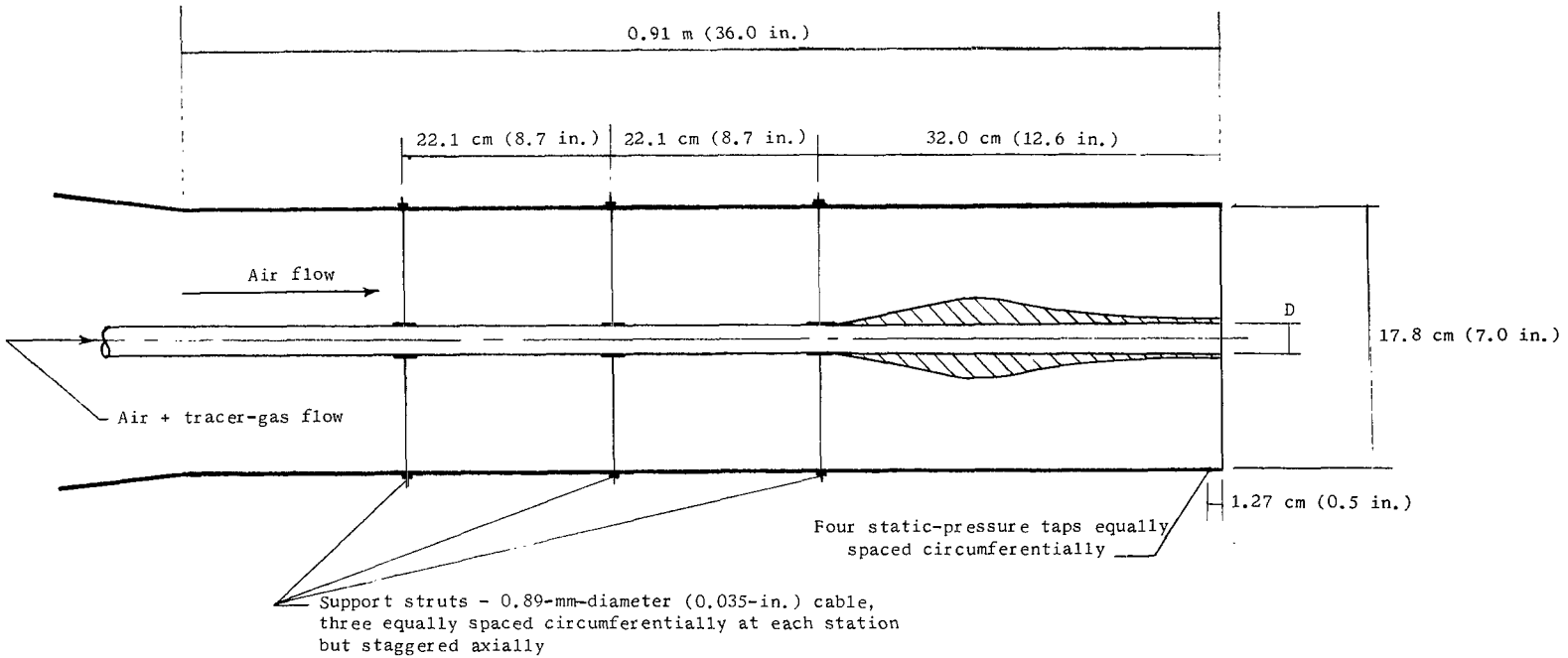

Central-nozzle inside diameter	Central-nozzle lip thickness	Outer-nozzle design Mach number	Central-nozzle design Mach number
2.443 cm (0.962 in.)	0.559 mm (0.022 in.)	1.3	Subsonic
1.036 cm (0.408 in.)	0.534 mm (0.021 in.)	1.3	Subsonic

Figure 1.- Sketch of nozzle test section.

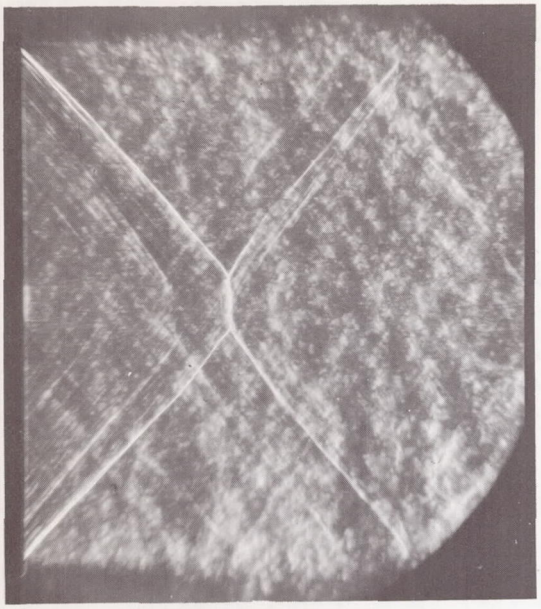

(a) Knife edge normal to flow; D = 1.036 cm (0.408 in.); M_j = 0.81; M_e = 1.27.

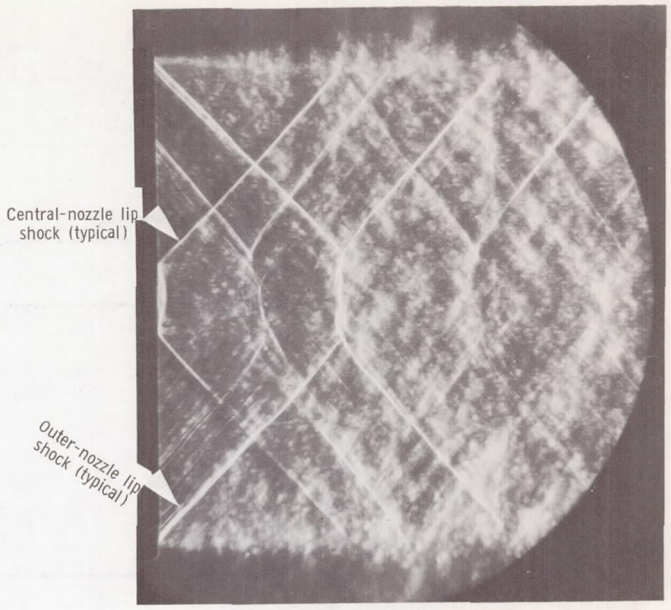

(b) Knife edge normal to flow; D = 2.443 cm (0.962 in.); M_j = 0.94; M_e = 1.30.

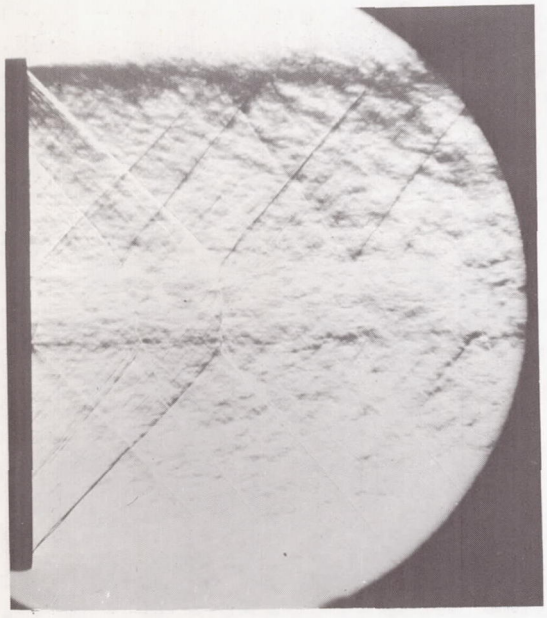

(c) Knife edge parallel to flow; D = 2.443 cm (0.962 in.); M_j = 0.94; M_e = 1.30.

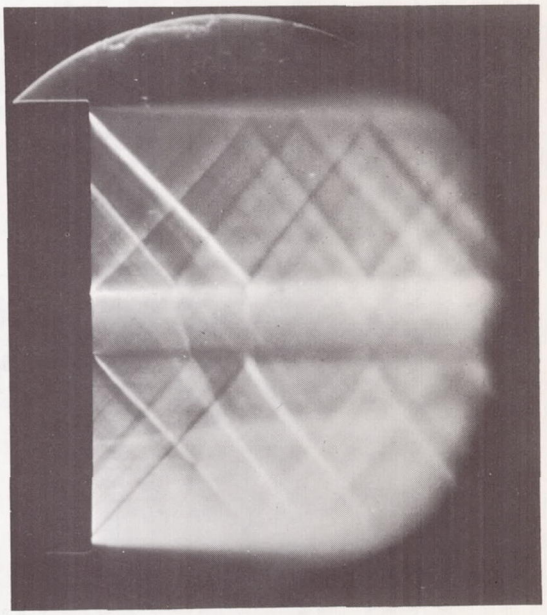

(d) Knife edge parallel to flow, time exposure; D = 2.443 cm (0.962 in.); M_j = 0.94; M_e = 1.30.

Figure 2.- Schlieren photographs of flow fields.

L-69-1384

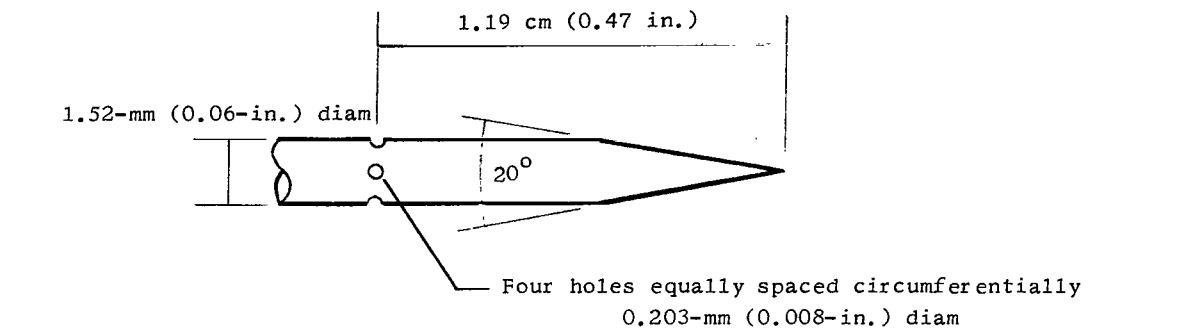

Static probe

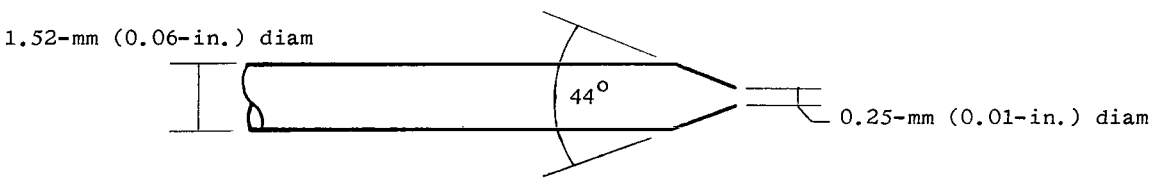

Pitot gas sampling probe

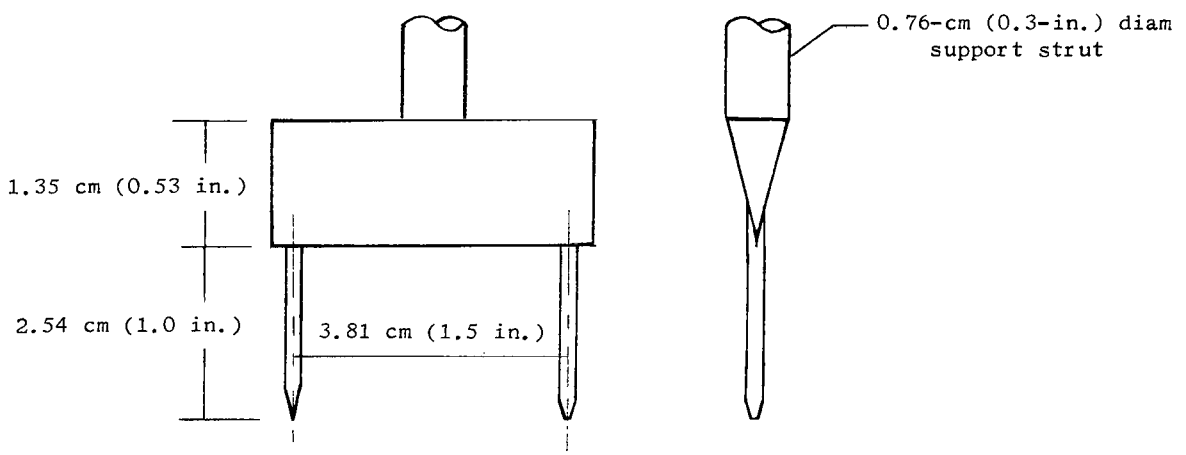

Survey rake

Figure 3.- Probes and survey rake.

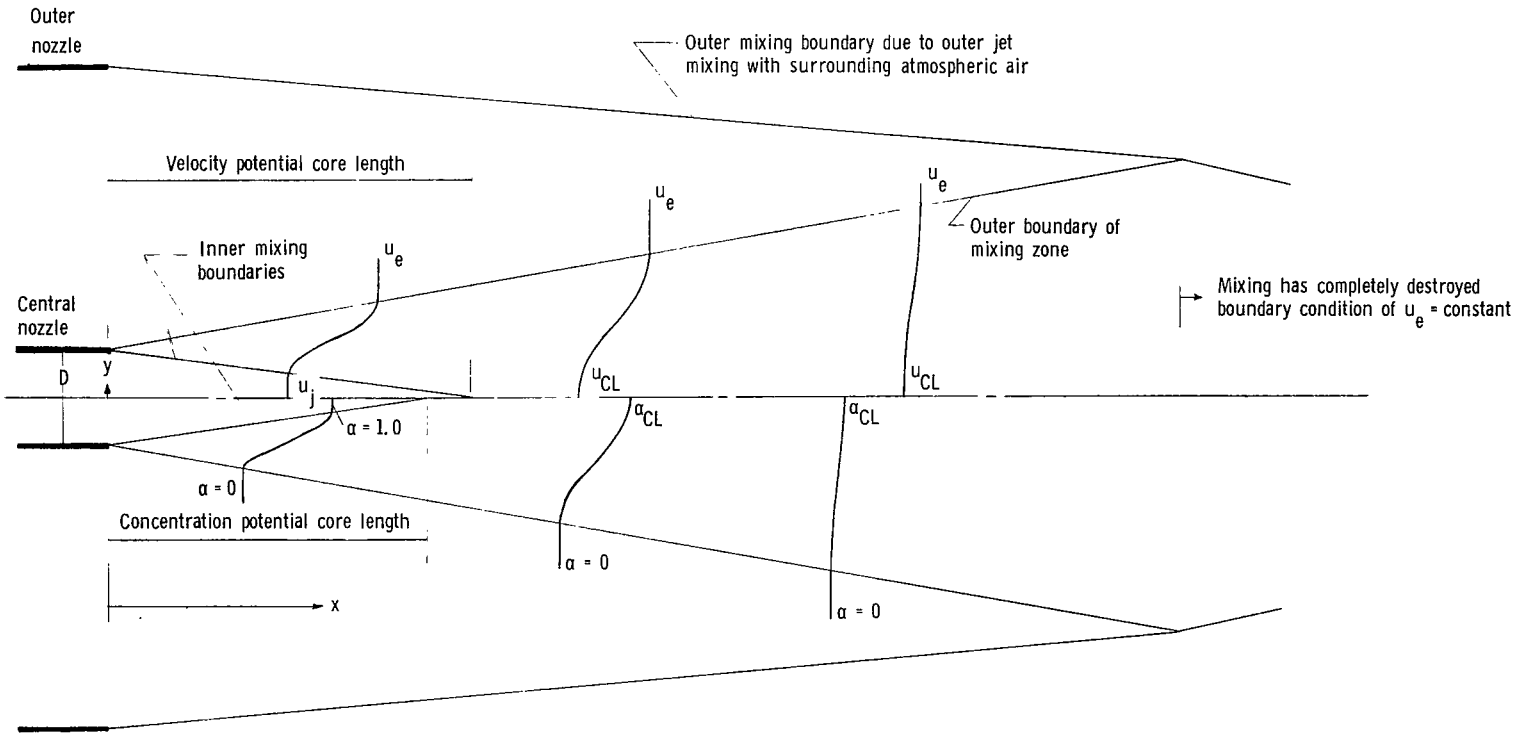

Figure 4.- Flow-field schematic.

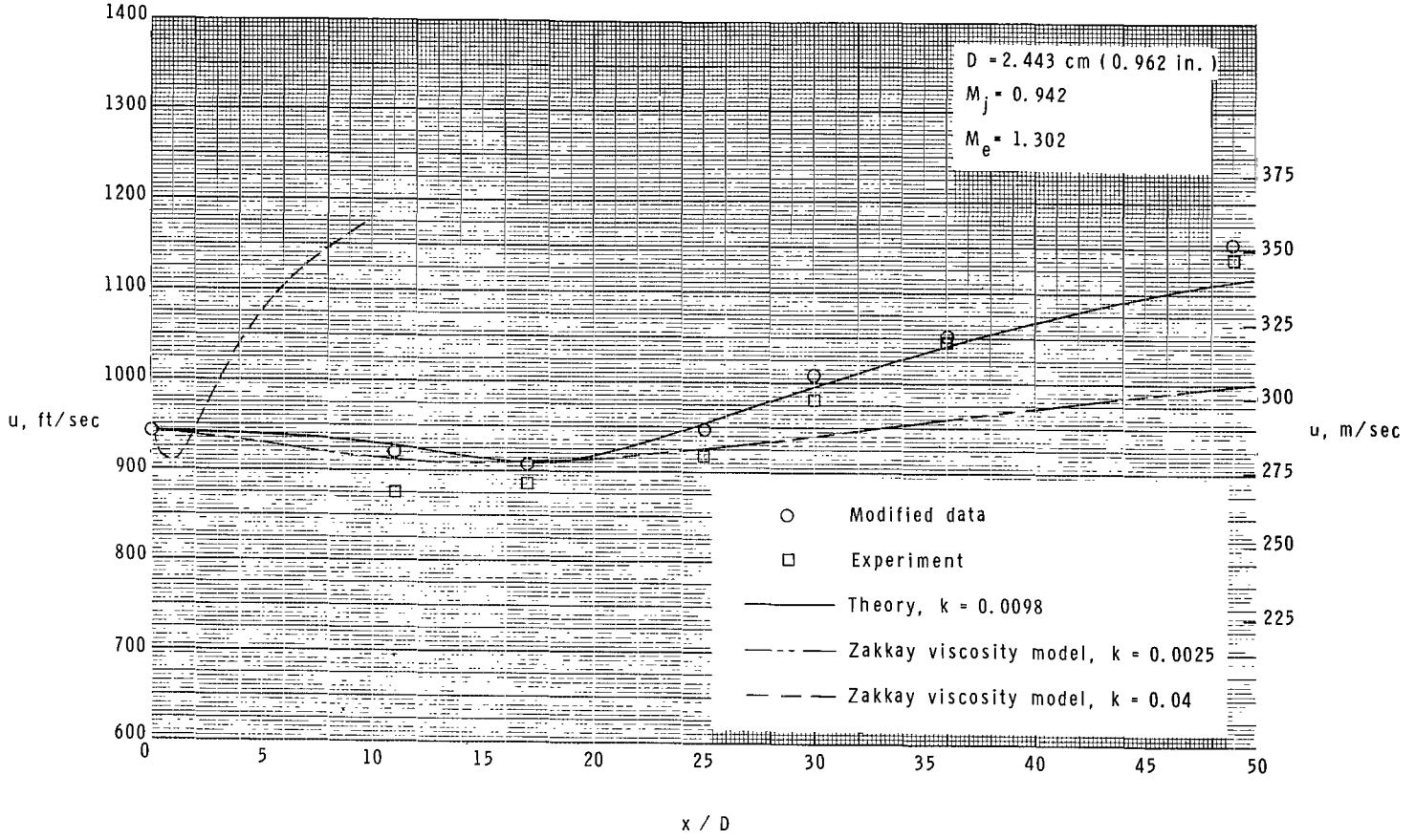

(a) Center-line velocity distribution.

Figure 5.- Data of test condition 1.

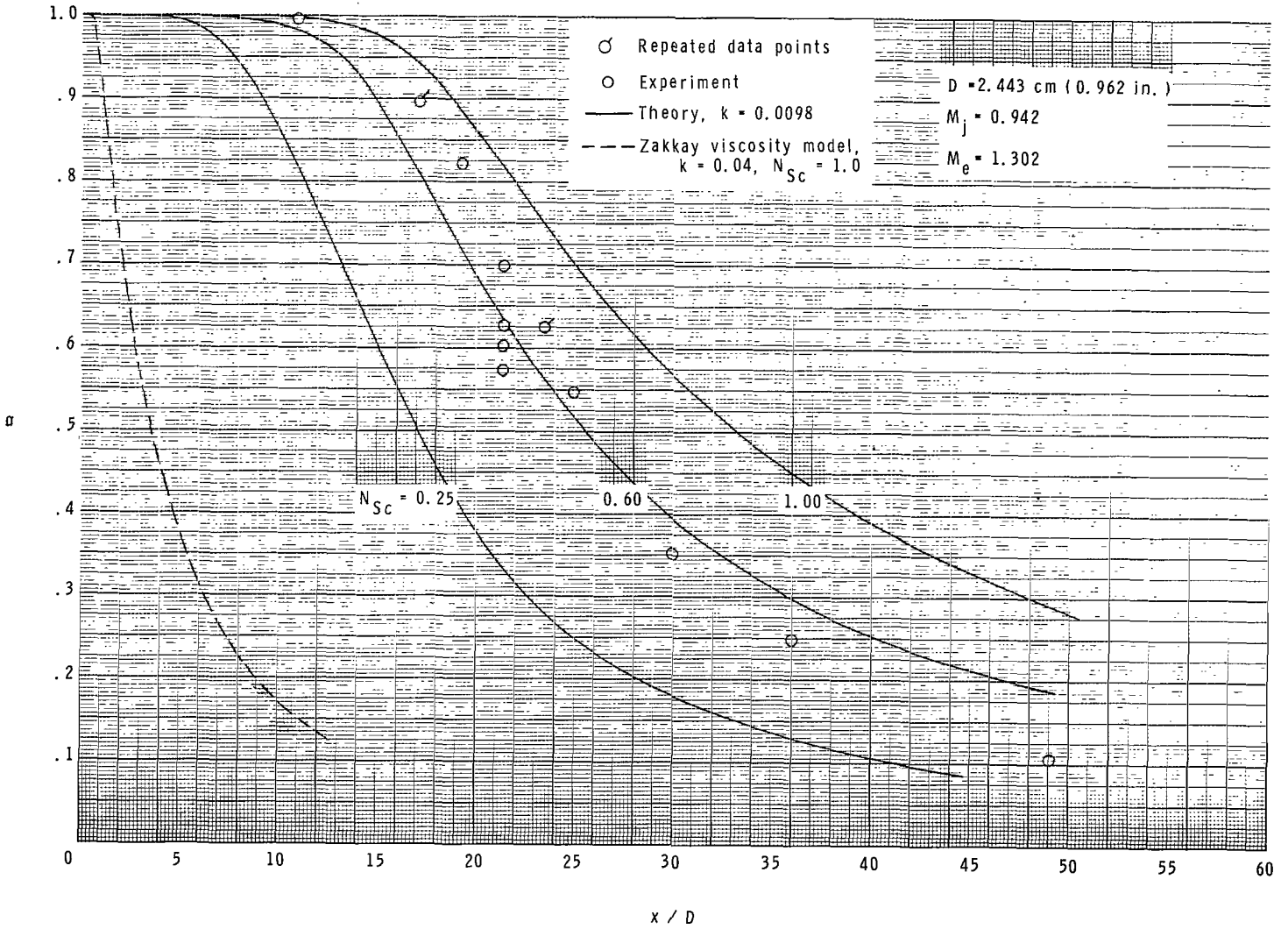

(b) Center-line concentration distribution.

Figure 5.- Continued.

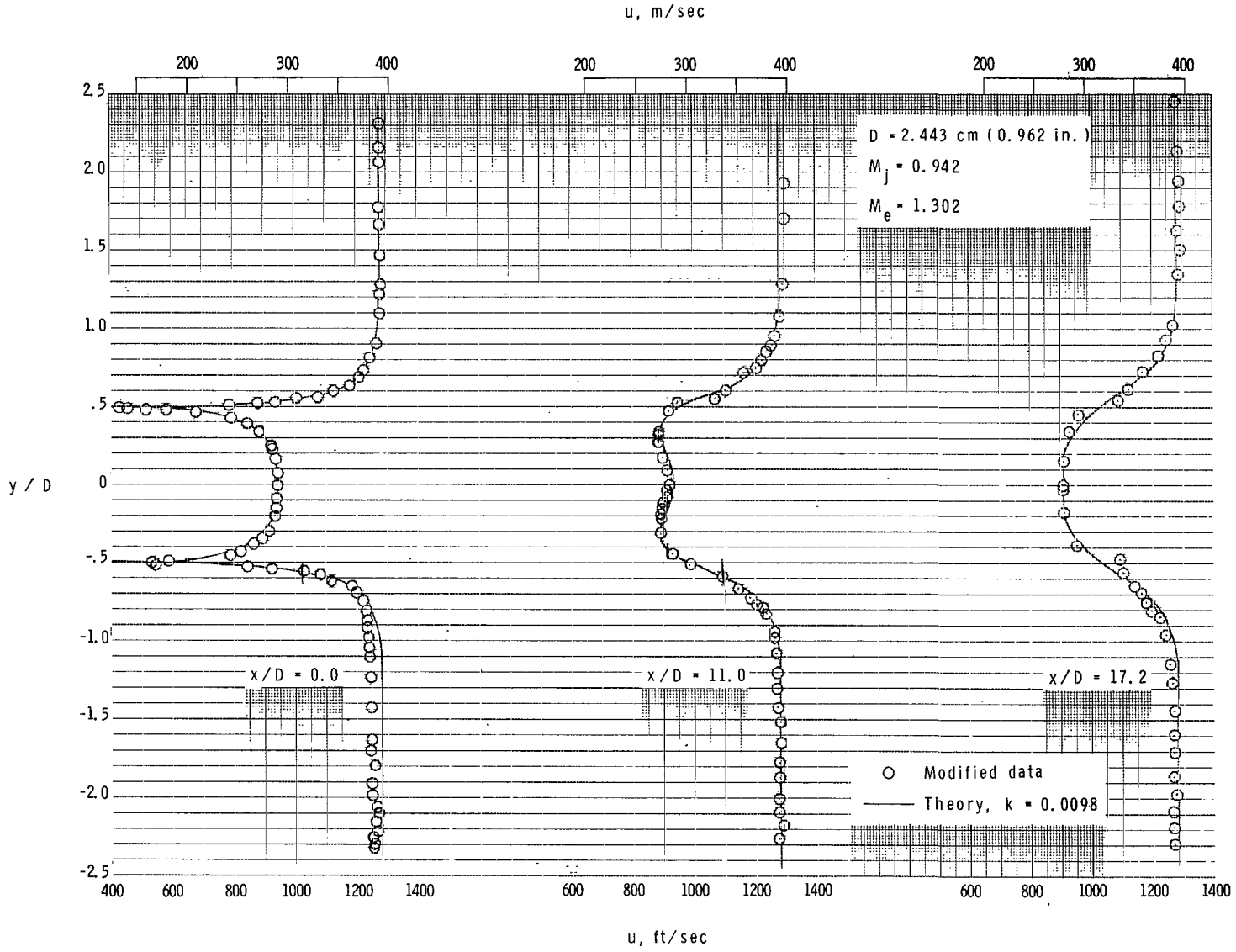

(c) Velocity profiles; x/D = 0.0 to 17.2.

Figure 5.- Continued.

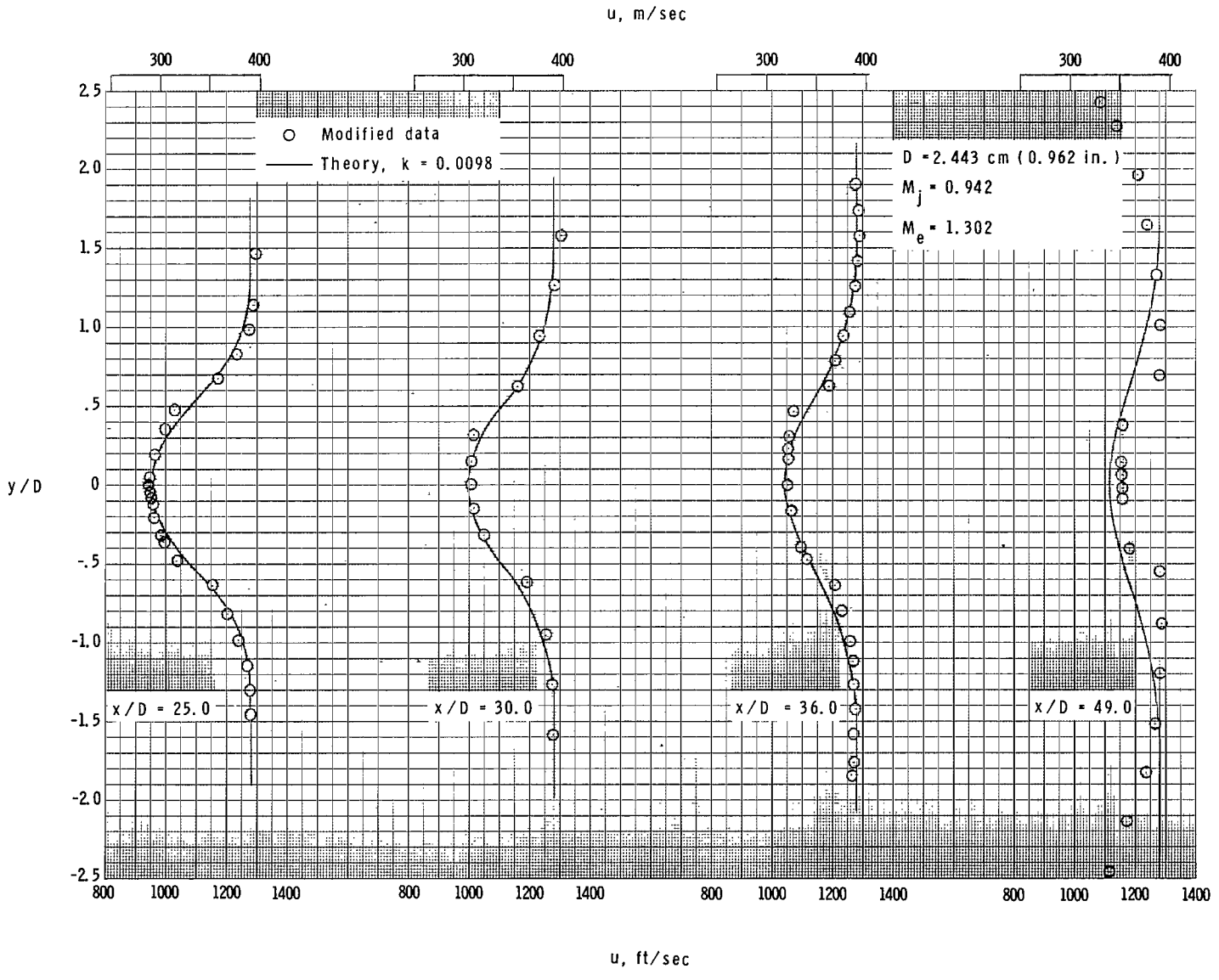

(d) Velocity profiles; x/D = 25.0 to 49.0.

Figure 5.- Continued.

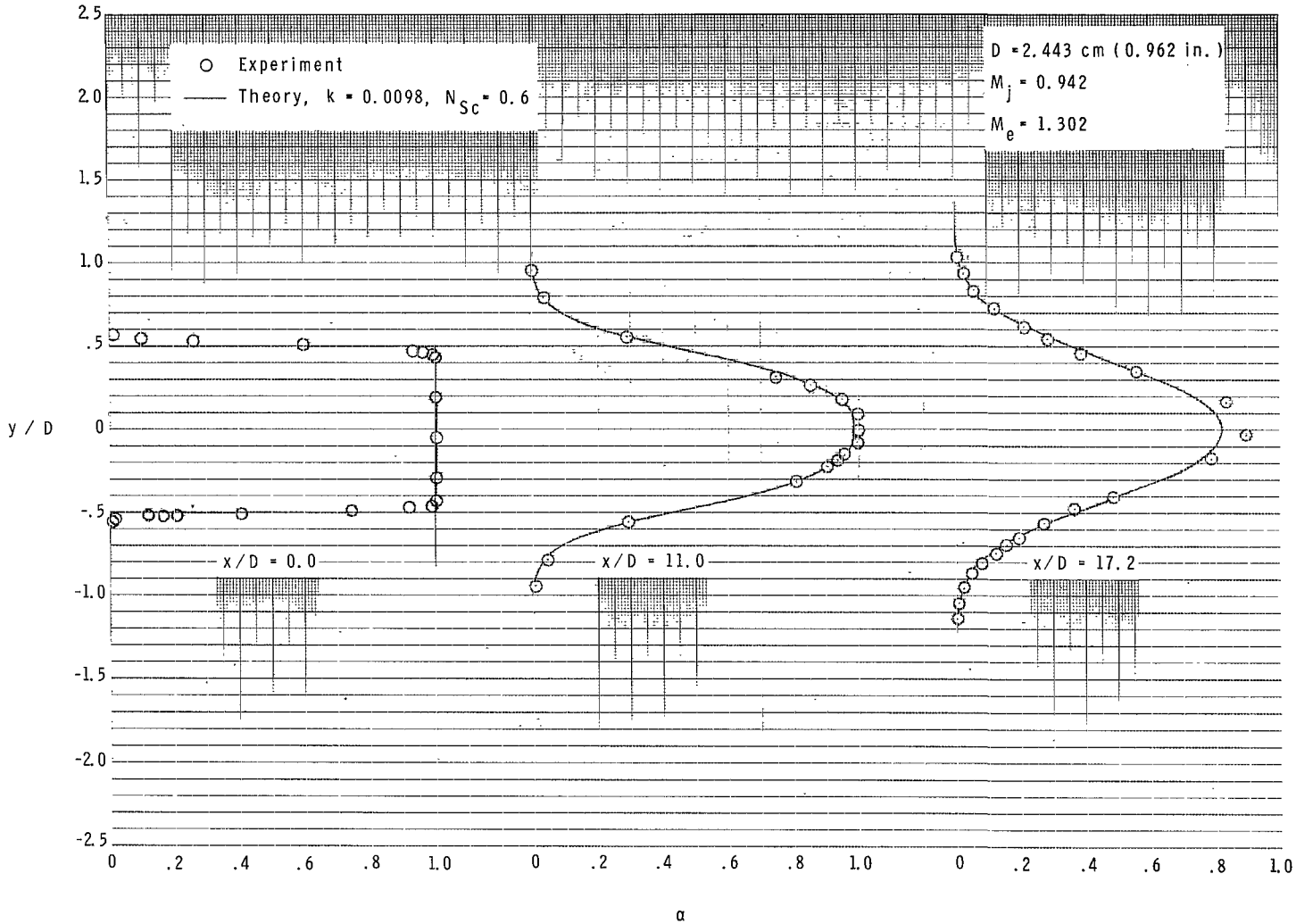

(e) Concentration profiles; x/D = 0.0 to 17.2.

Figure 5.- Continued.

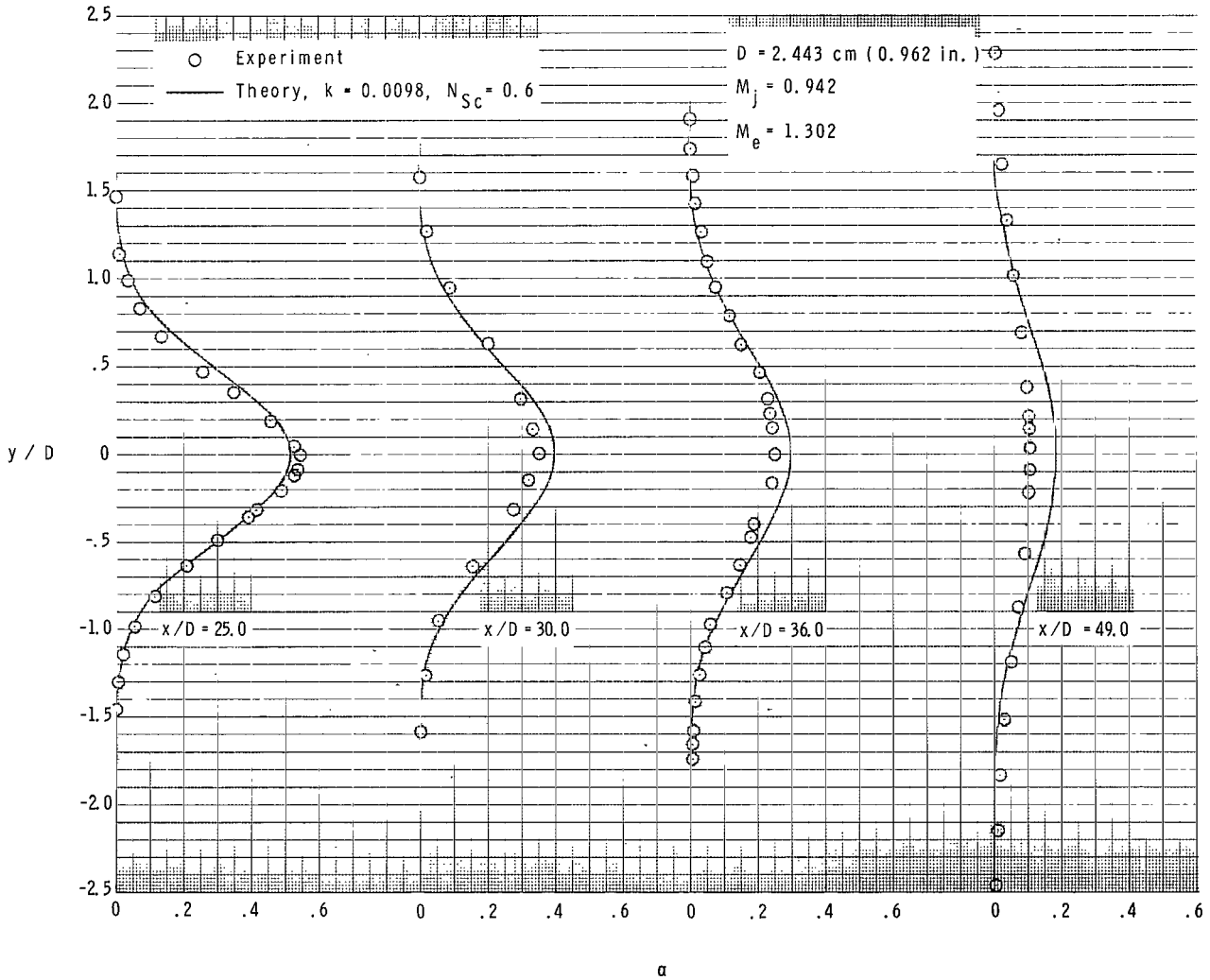

(f) Concentration profiles; x/D = 25.0 to 49.0.

Figure 5.- Concluded.

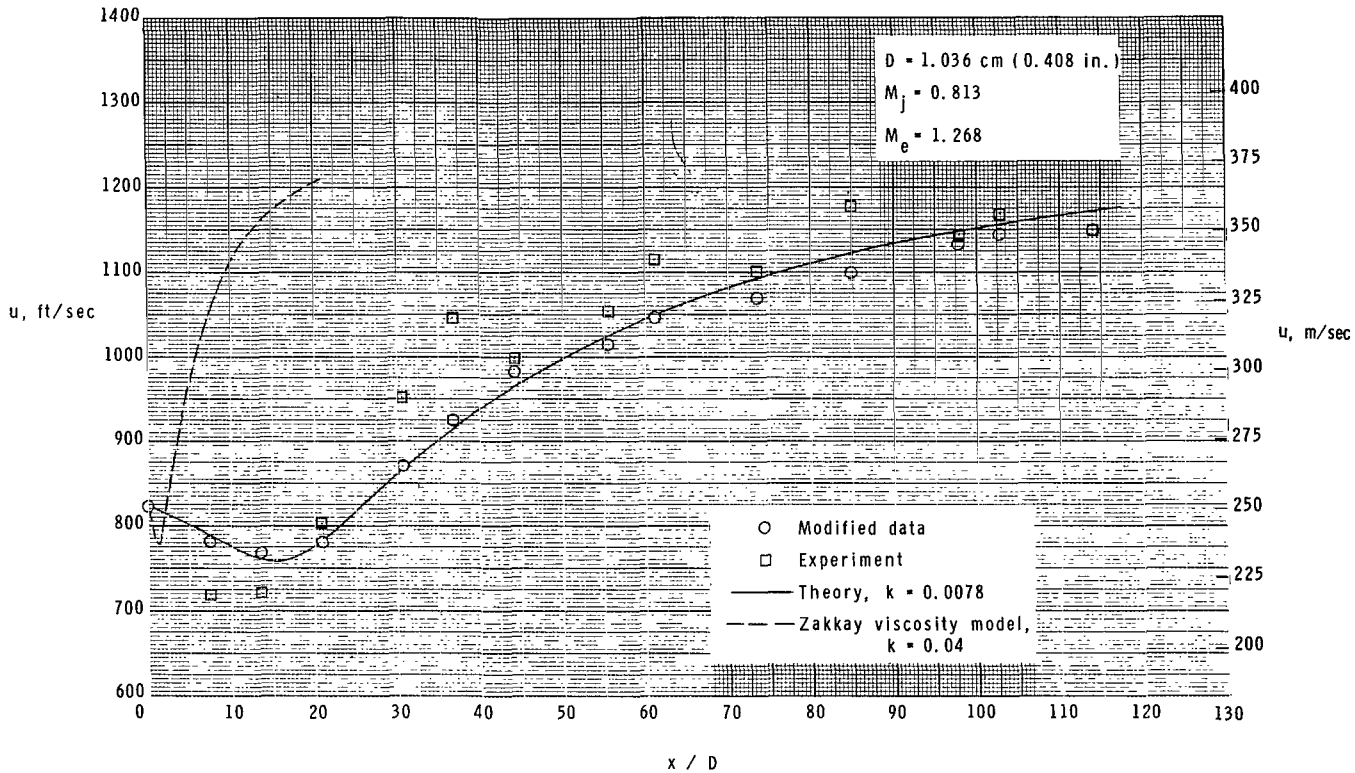

(a) Center-line velocity distributions.

Figure 6.- Data of test condition 2.

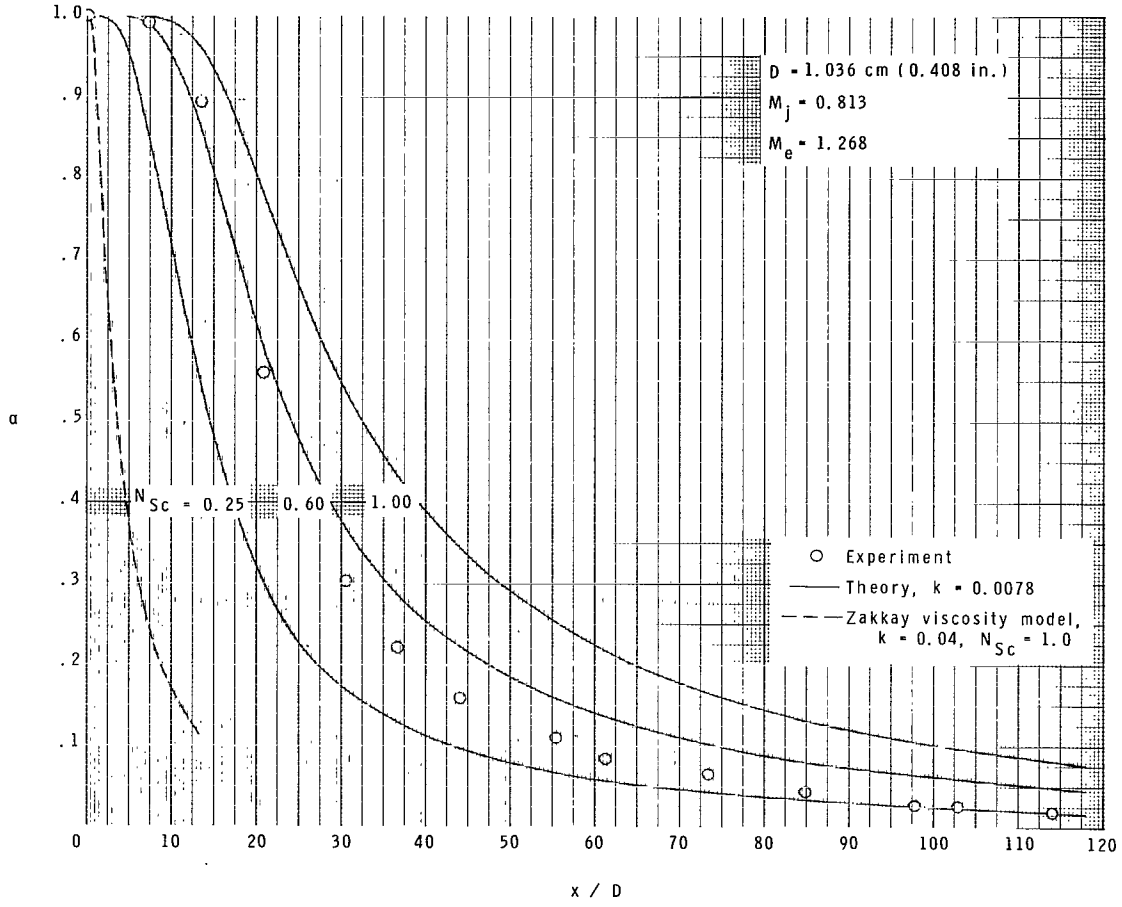

(b) Center-line concentration distributions.

Figure 6.- Continued.

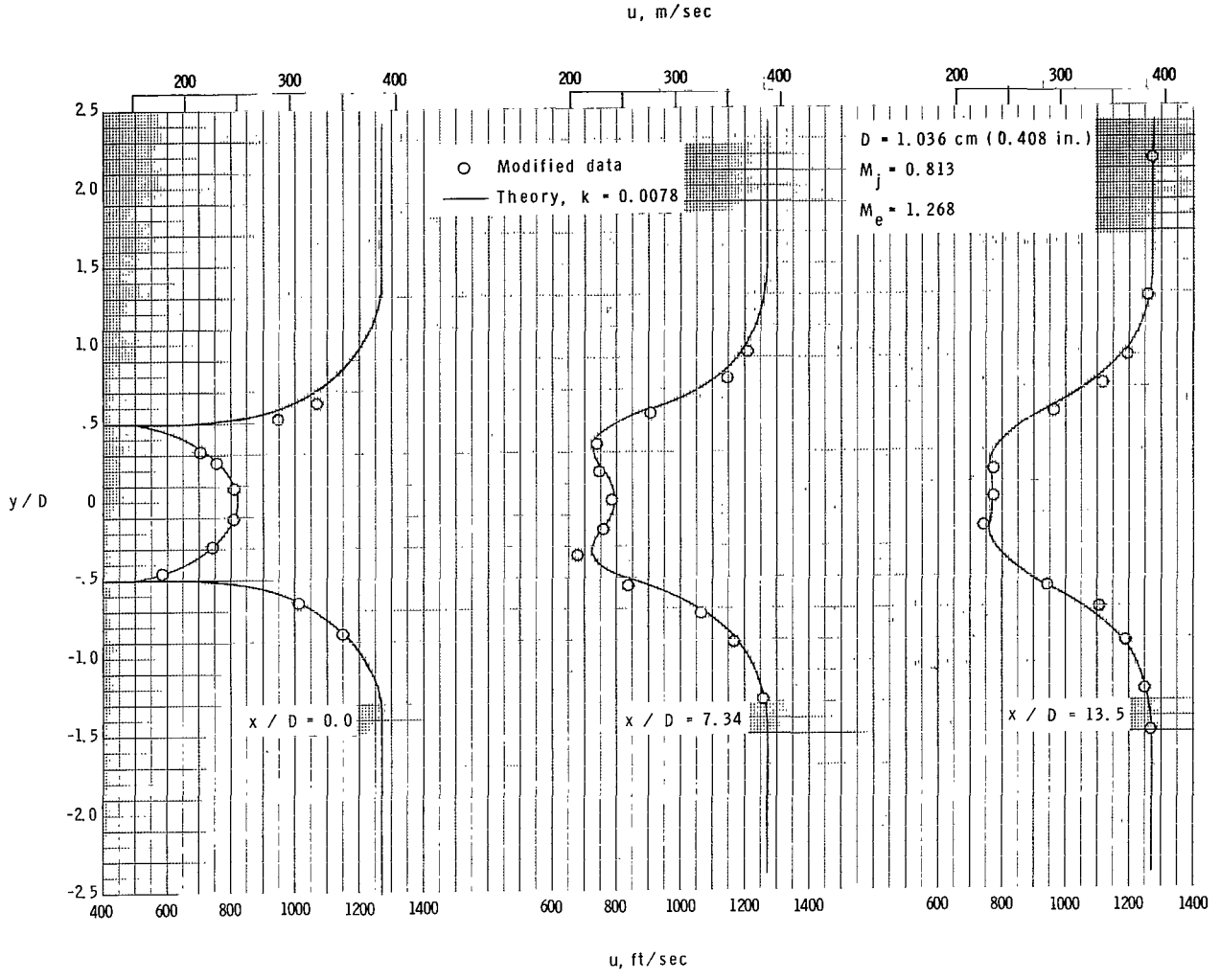

(c) Velocity profiles; x/D = 0.0 to 13.5.

Figure 6.- Continued.

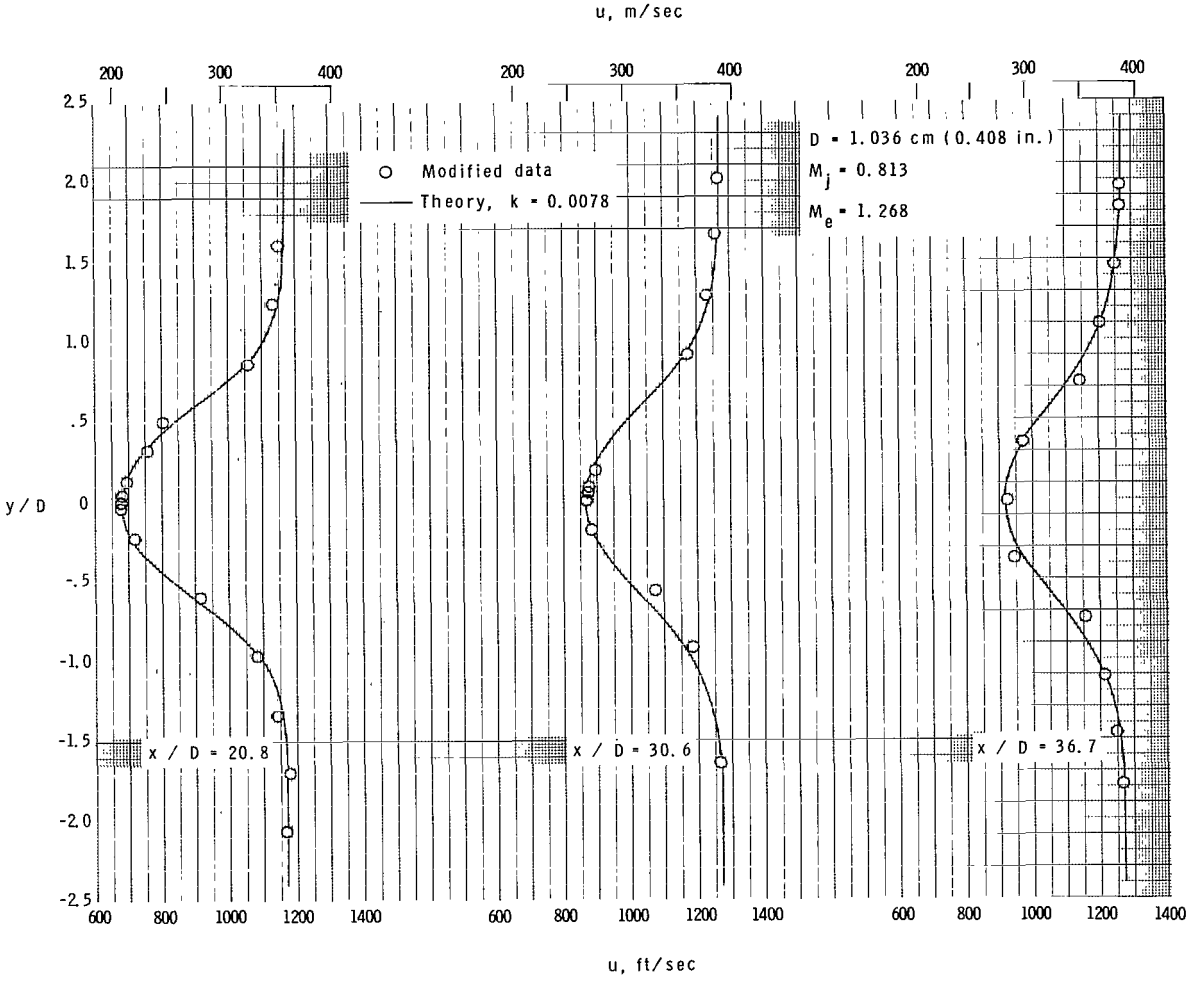

(d) Velocity profiles; x/D = 20.8 to 36.7.

Figure 6.- Continued.

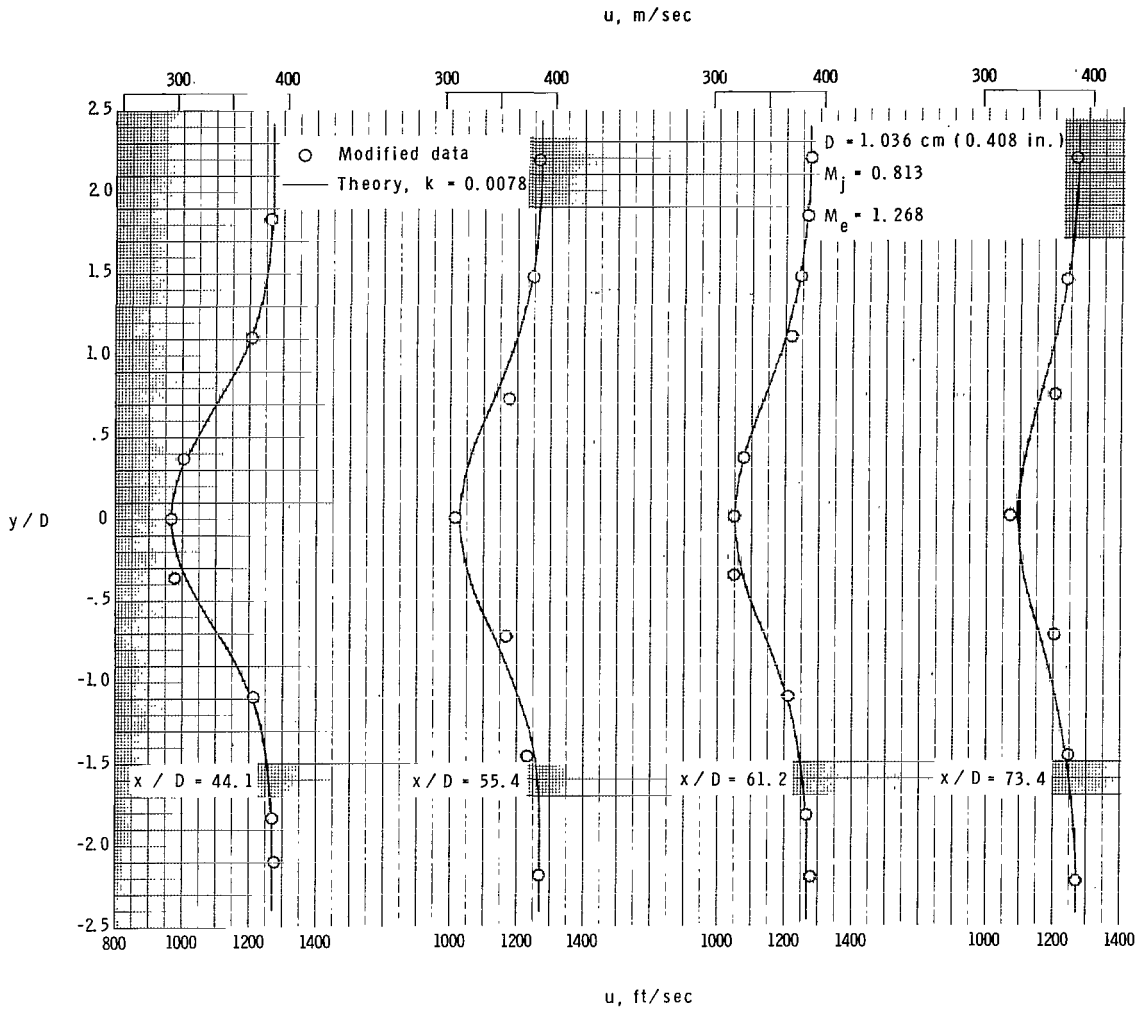

(e) Velocity profiles; x/D = 44.1 to 73.4.

Figure 6.- Continued.

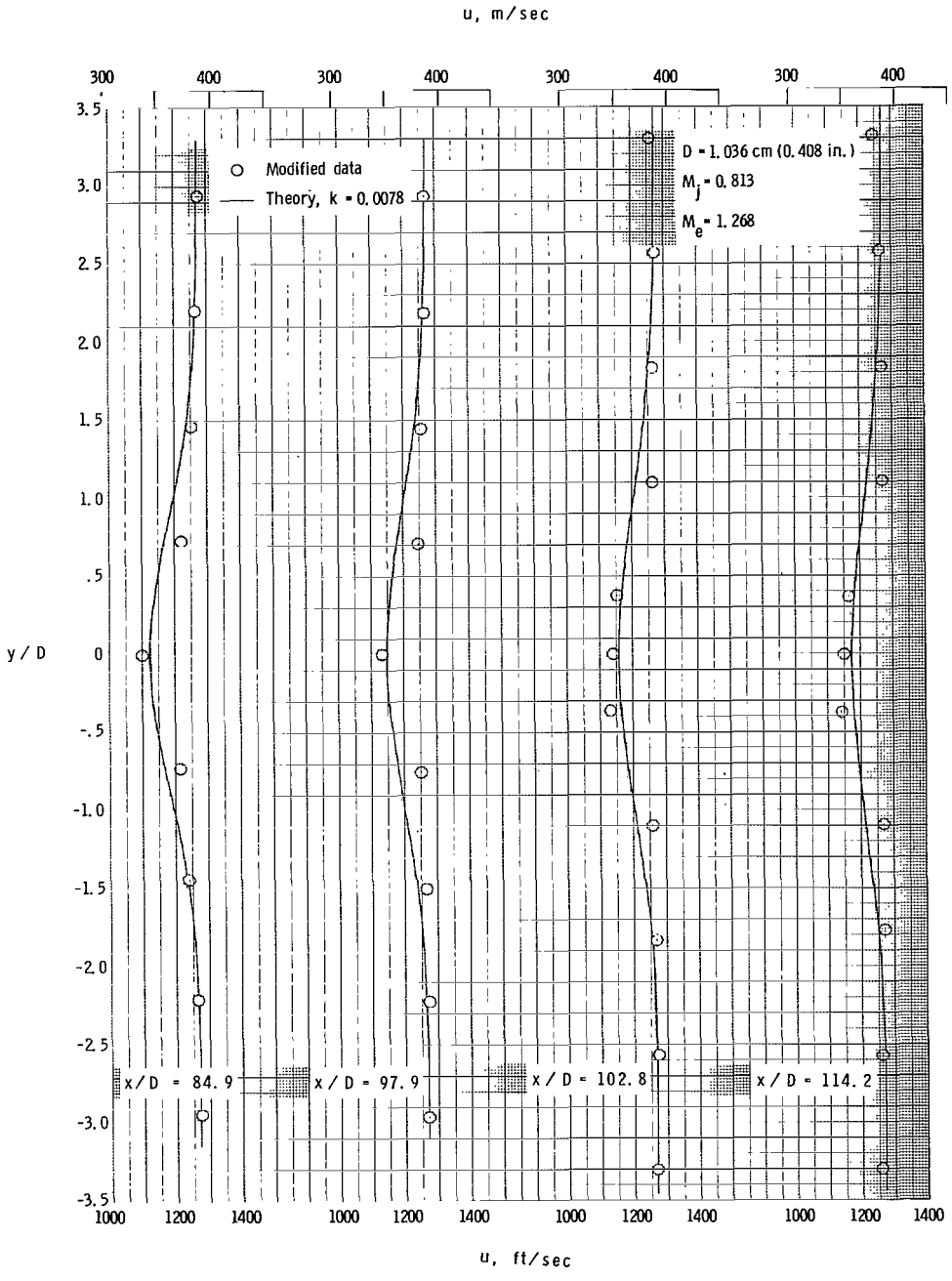

(f) Velocity profiles; x/D = 84.9 to 114.2.

Figure 6.- Continued.

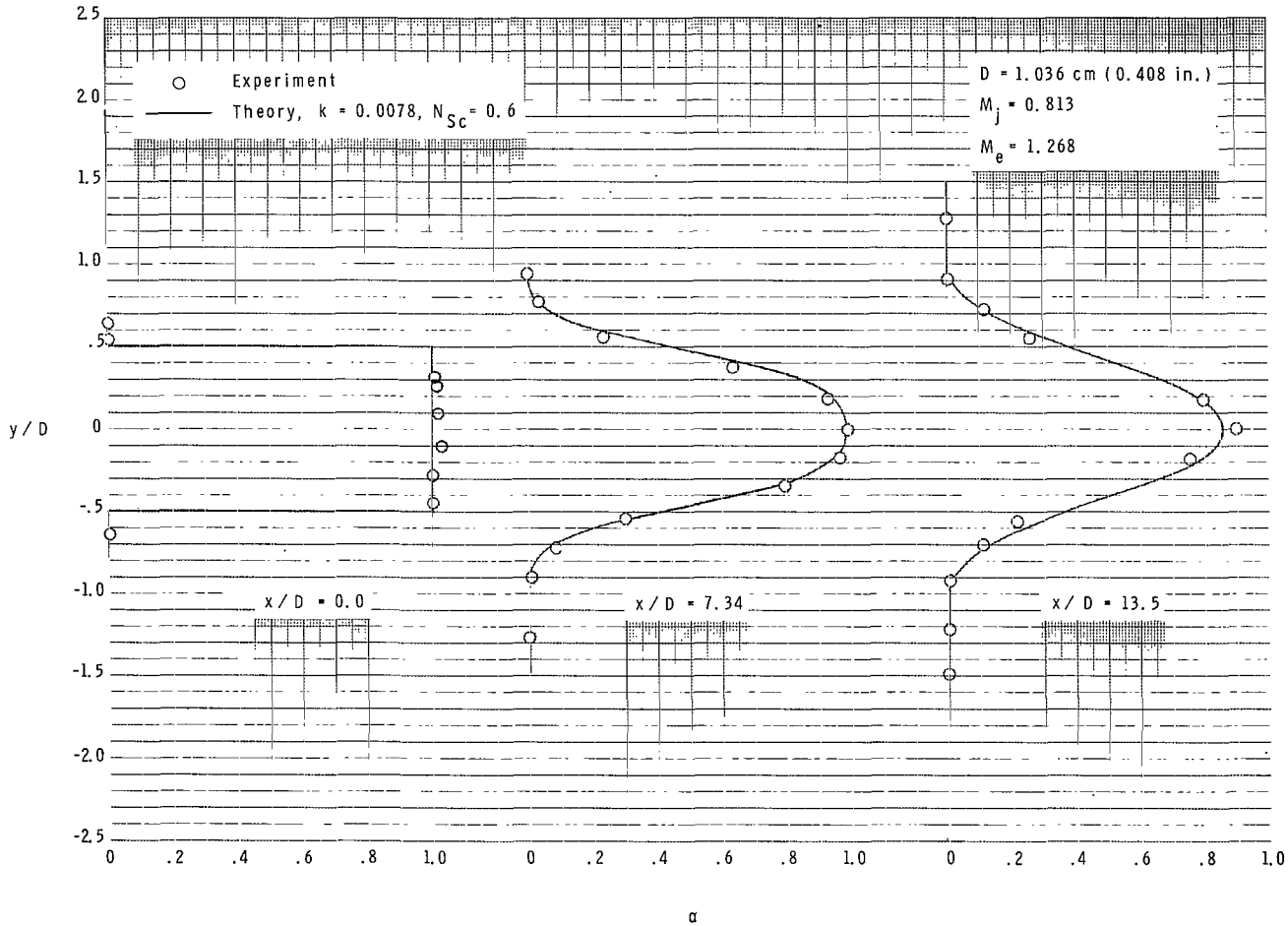

(g) Concentration profiles; x/D = 0.0 to 13.5.

Figure 6.- Continued.

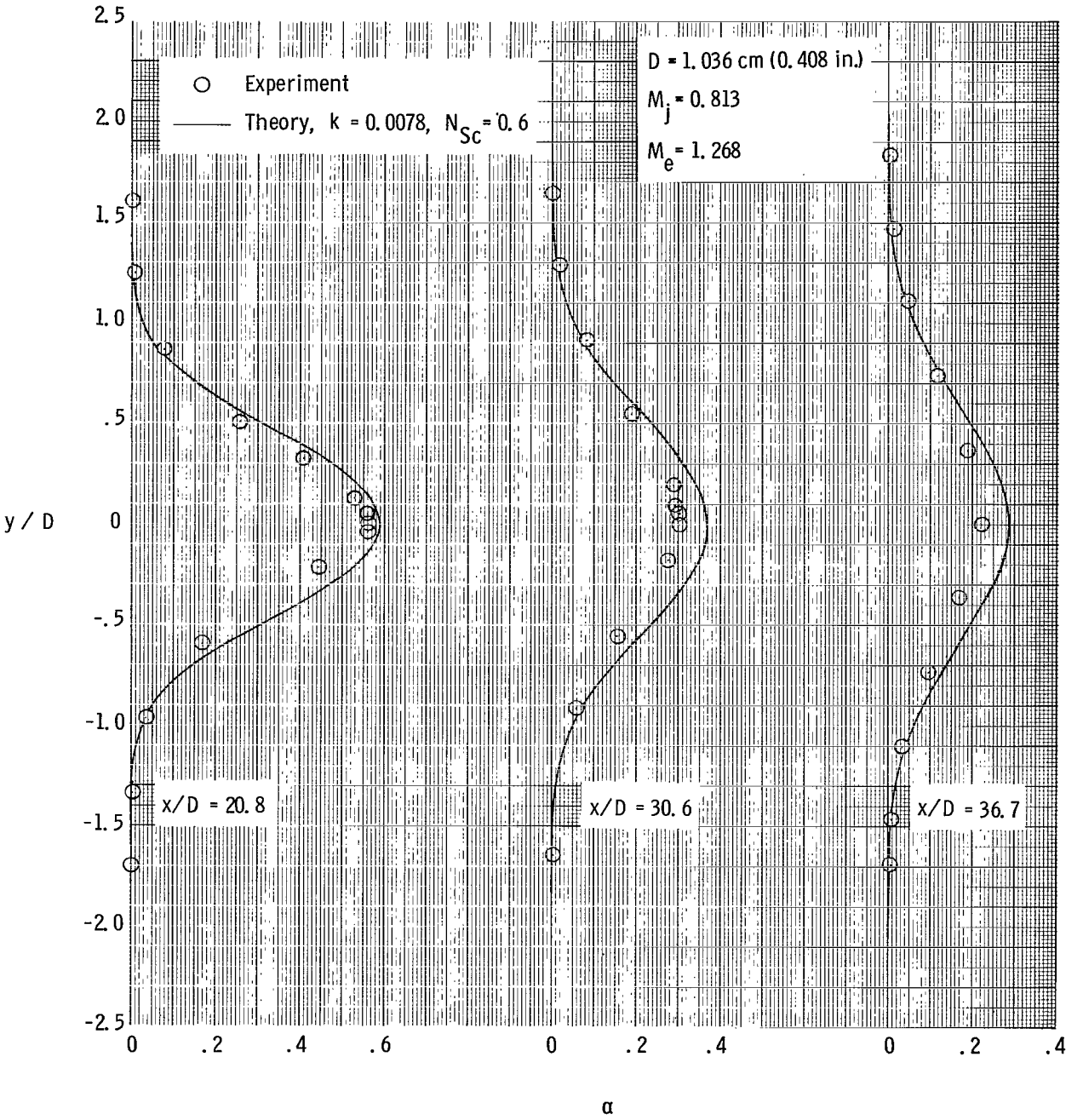

(h) Concentration profiles; x/D = 20.8 to 36.7.

Figure 6.- Continued.

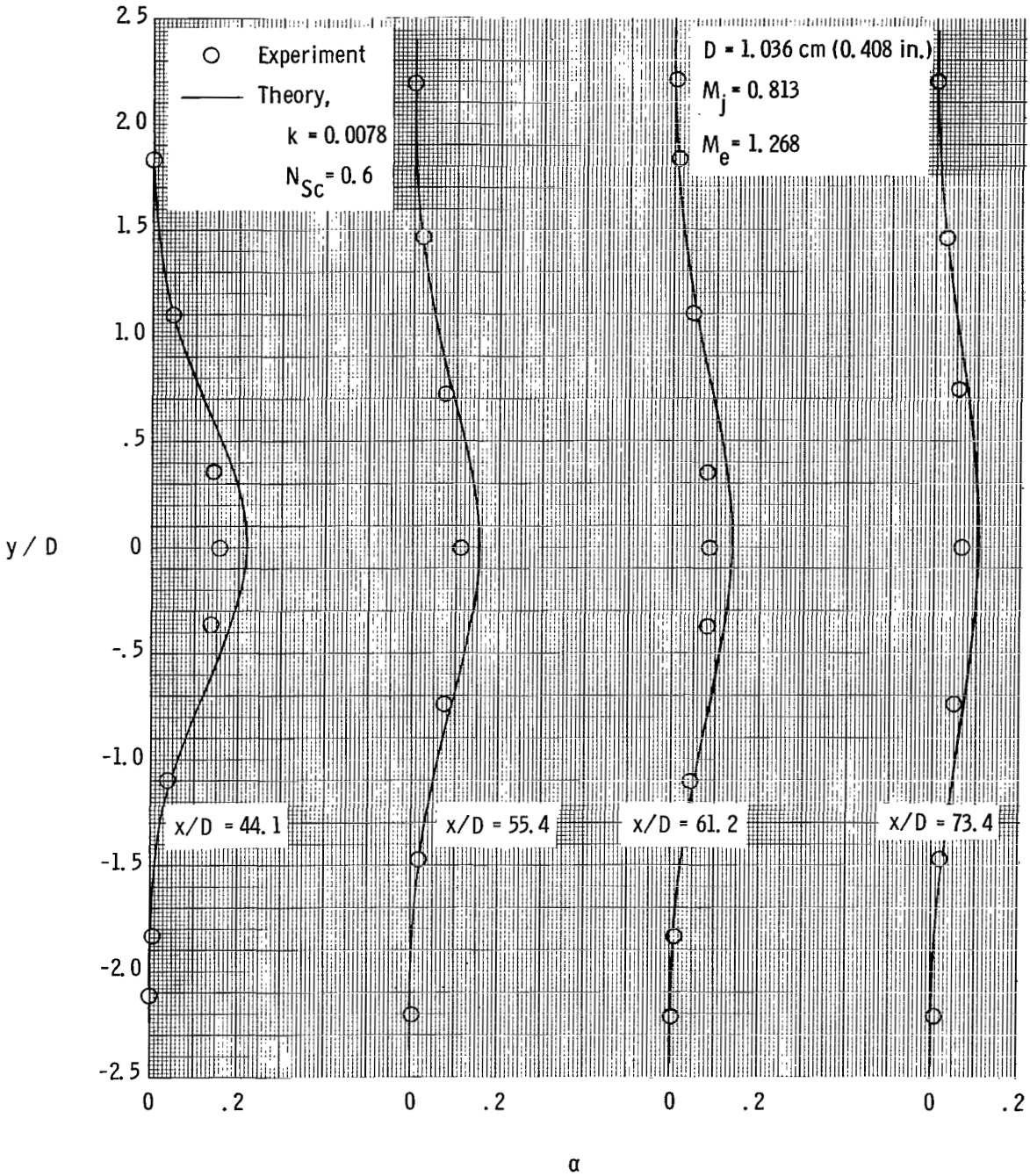

(i) Concentration profiles; x/D = 44.1 to 73.4.

Figure 6.- Continued.

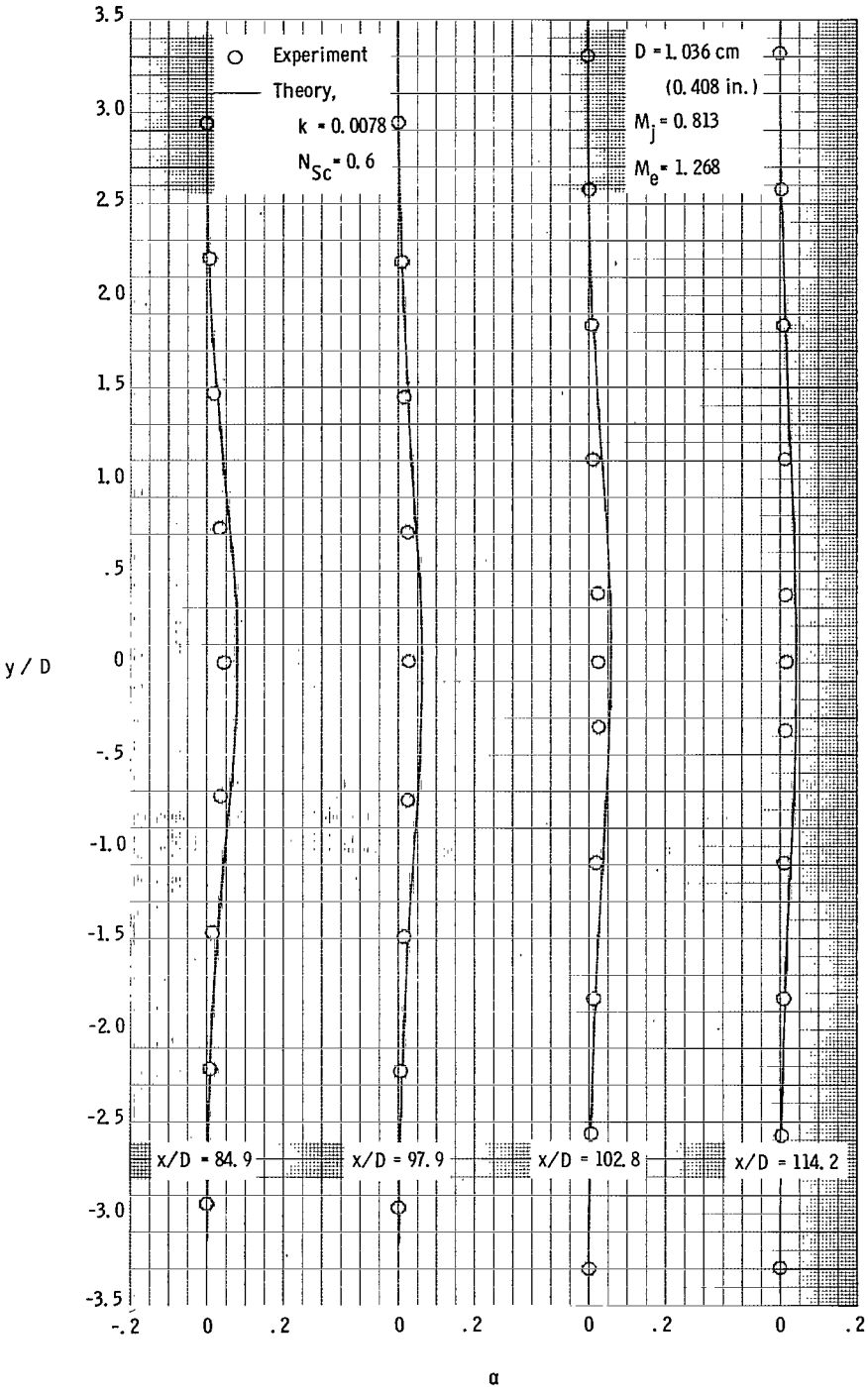

(j) Concentration profiles; x/D = 84.9 to 114.2.

Figure 6.- Concluded.

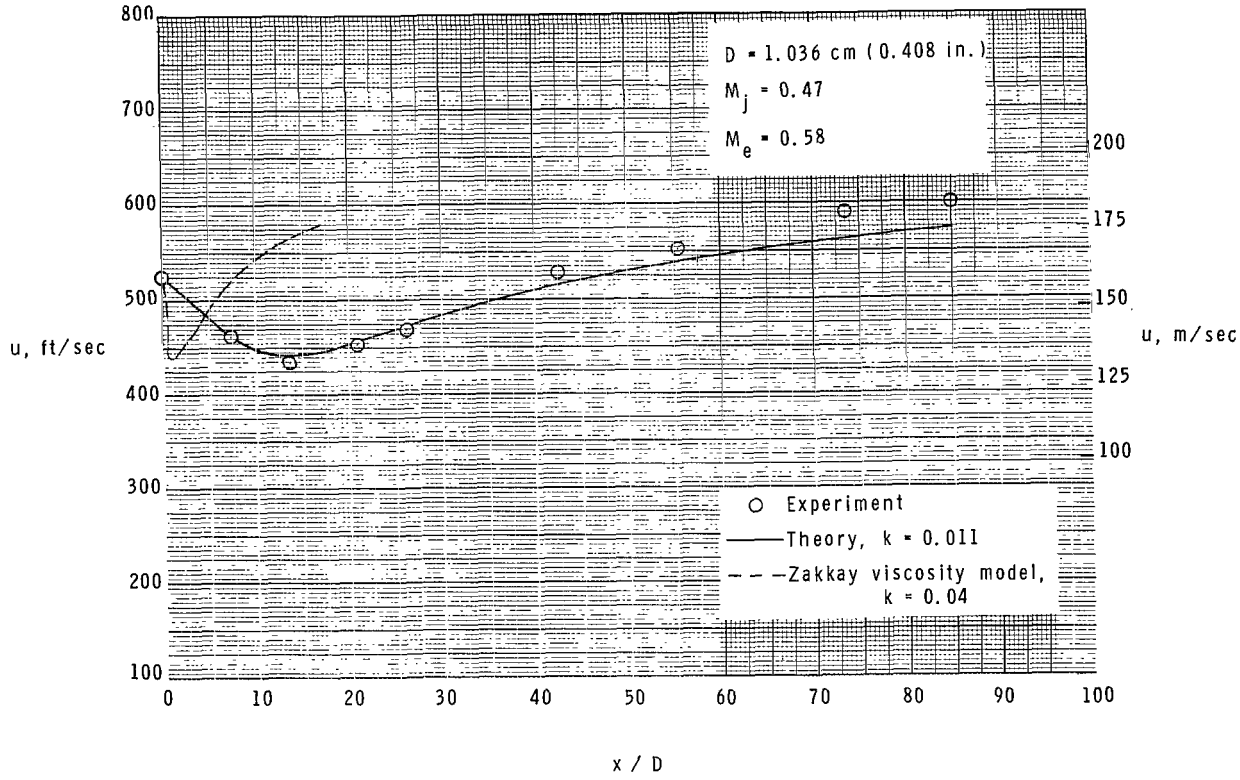

(a) Center-line velocity distribution.

Figure 7.- Data of test condition 3.

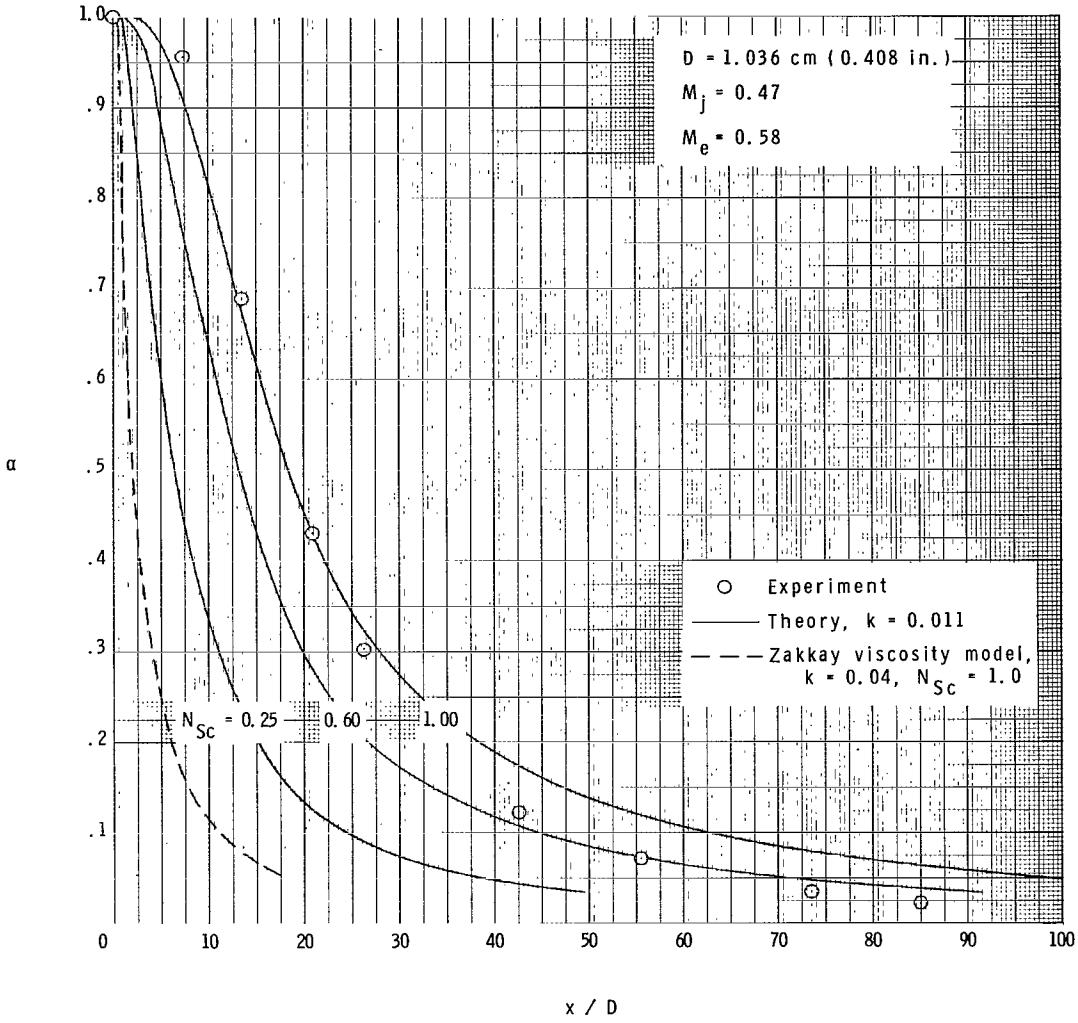

(b) Center-line concentration distribution.

Figure 7.- Continued.

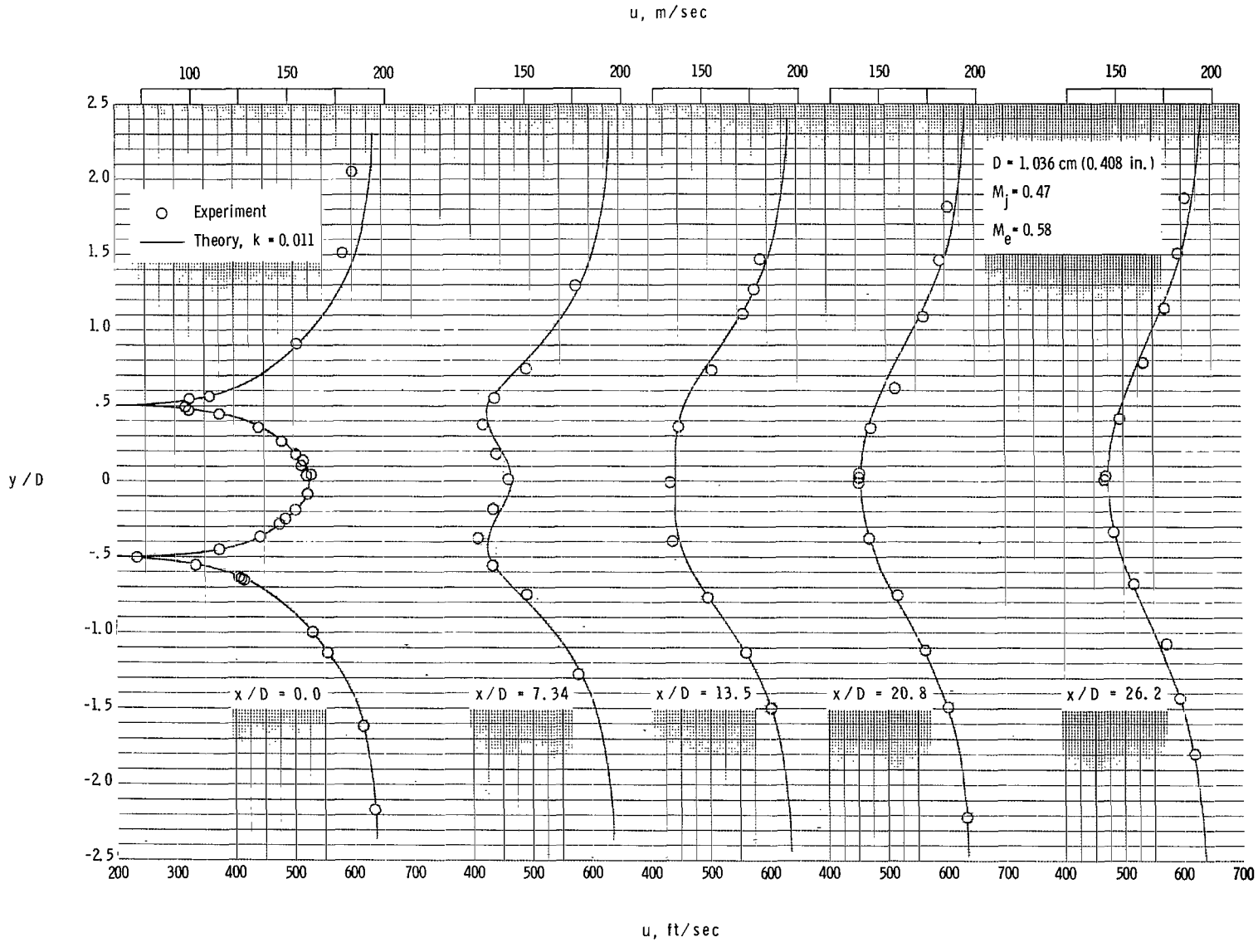

(c) Velocity profiles; x/D = 0.0 to 26.2.

Figure 7.- Continued.

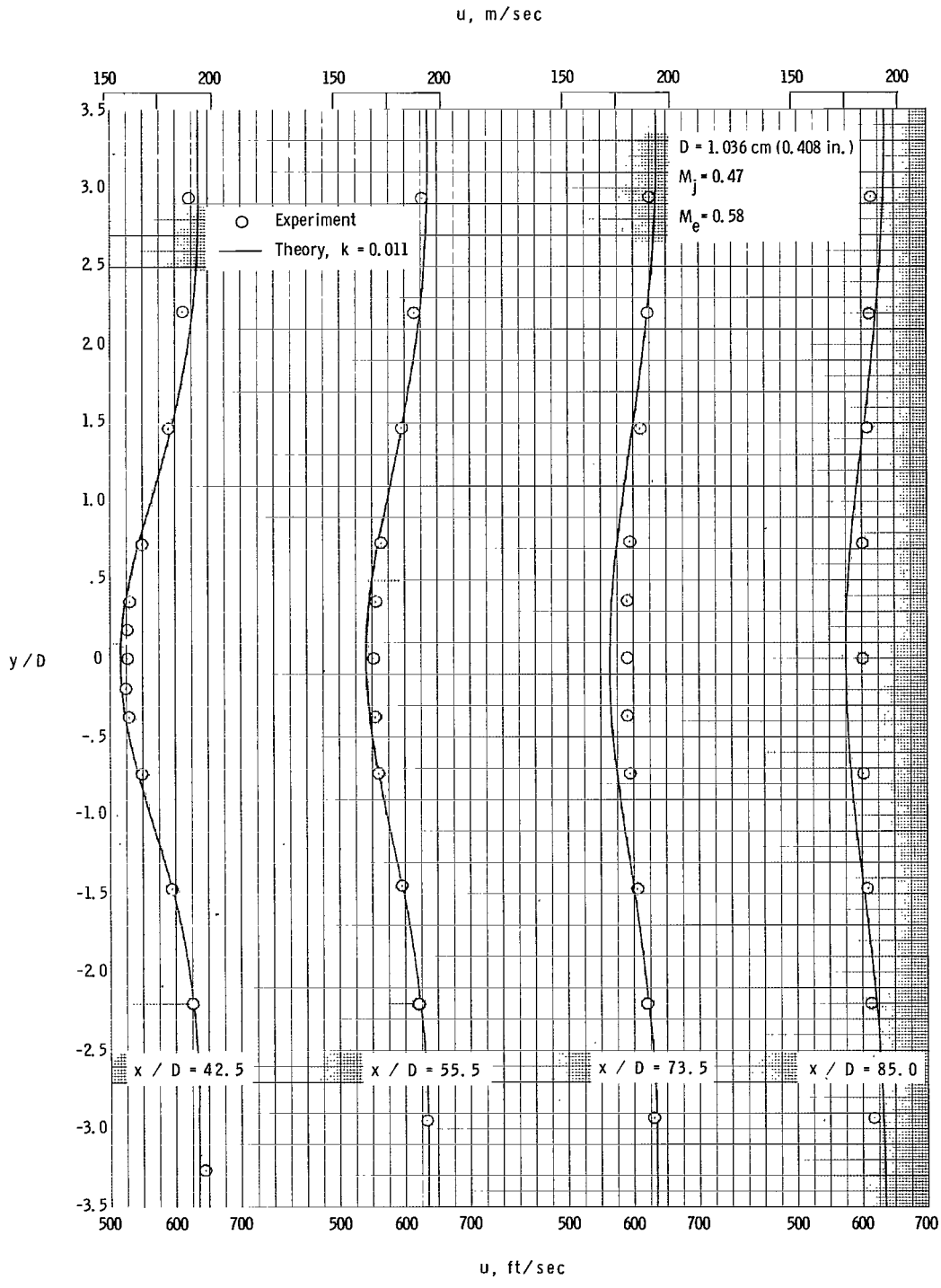

(d) Velocity profiles; x/D = 42.5 to 85.0.

Figure 7.- Continued.

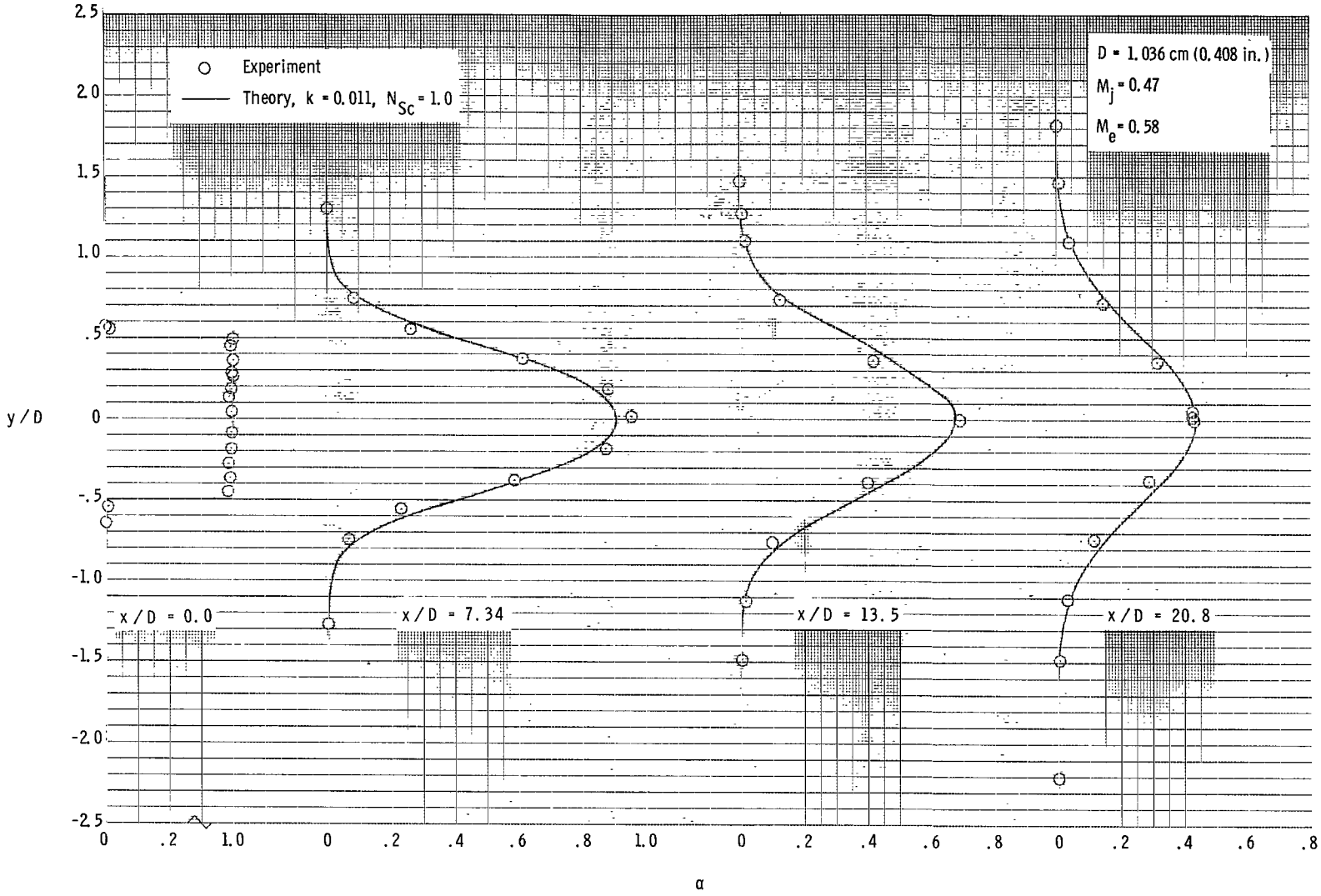

(e) Concentration profiles; x/D = 0.0 to 20.8.

Figure 7.- Continued.

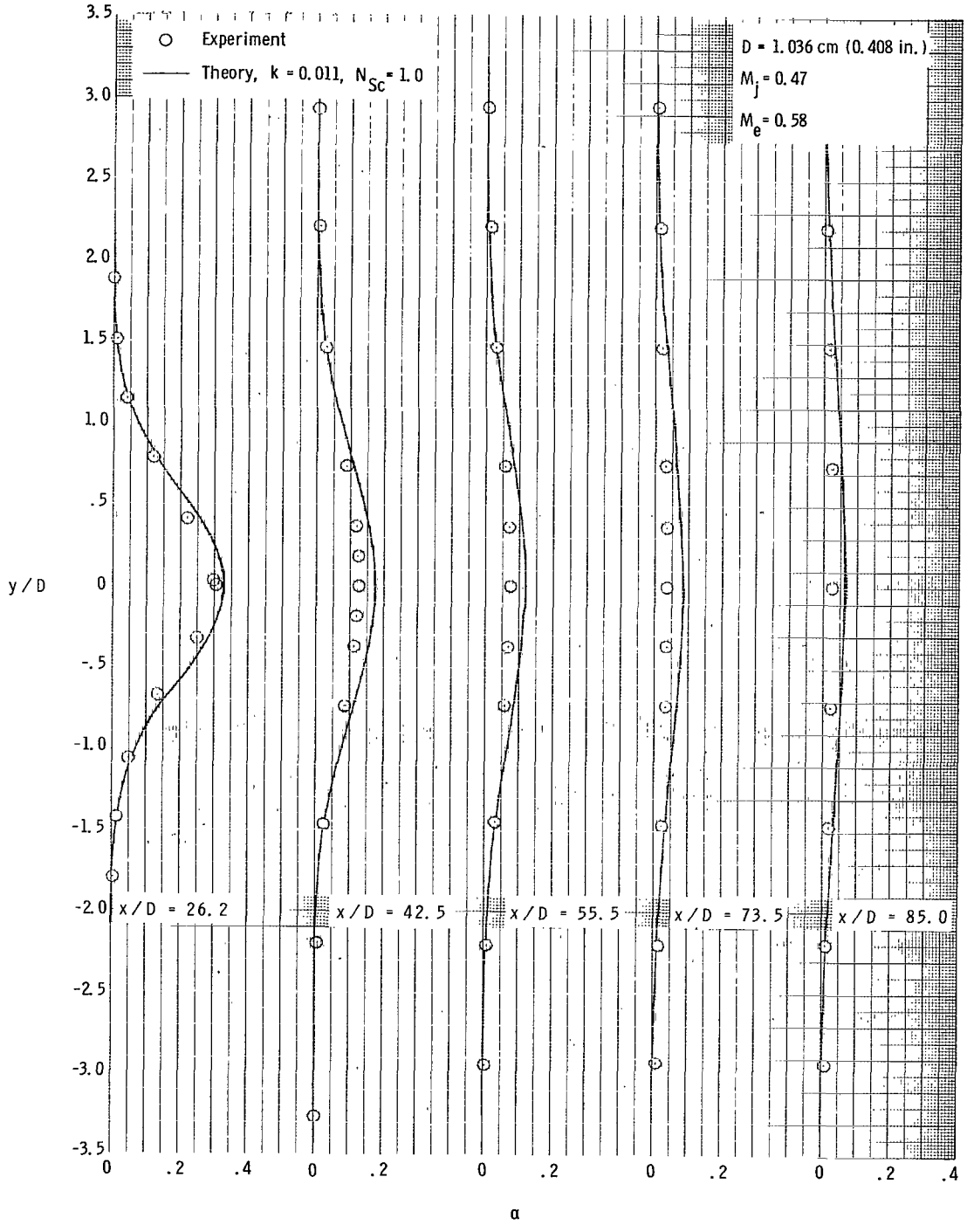

(f) Concentration profiles; x/D = 26.2 to 85.0.

Figure 7.- Concluded.

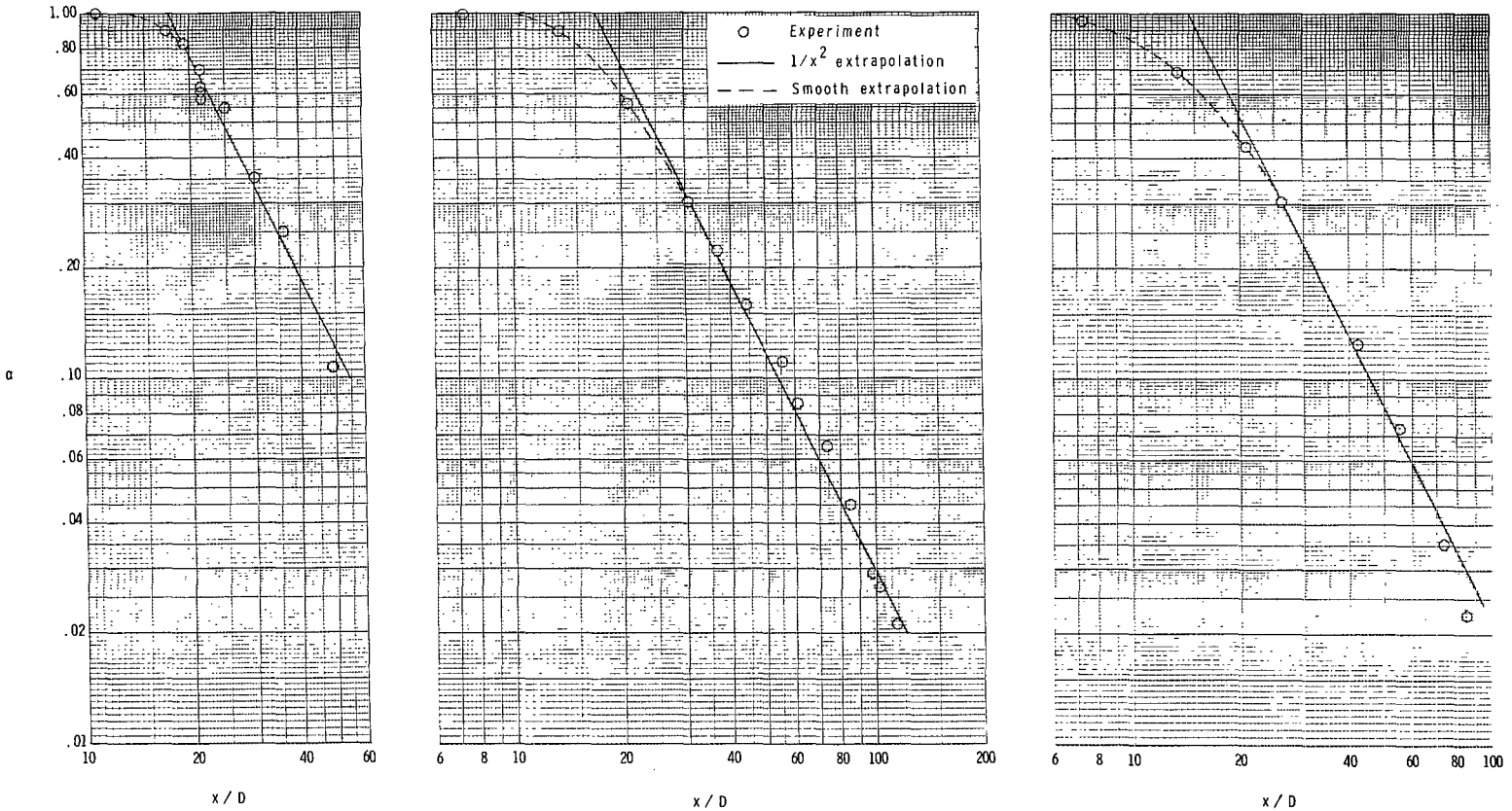

(a) Test condition 1. (b) Test condition 2. (c) Test condition 3.

Figure 8.- Center-line concentrations compared with a decay inversely proportional to x^2.

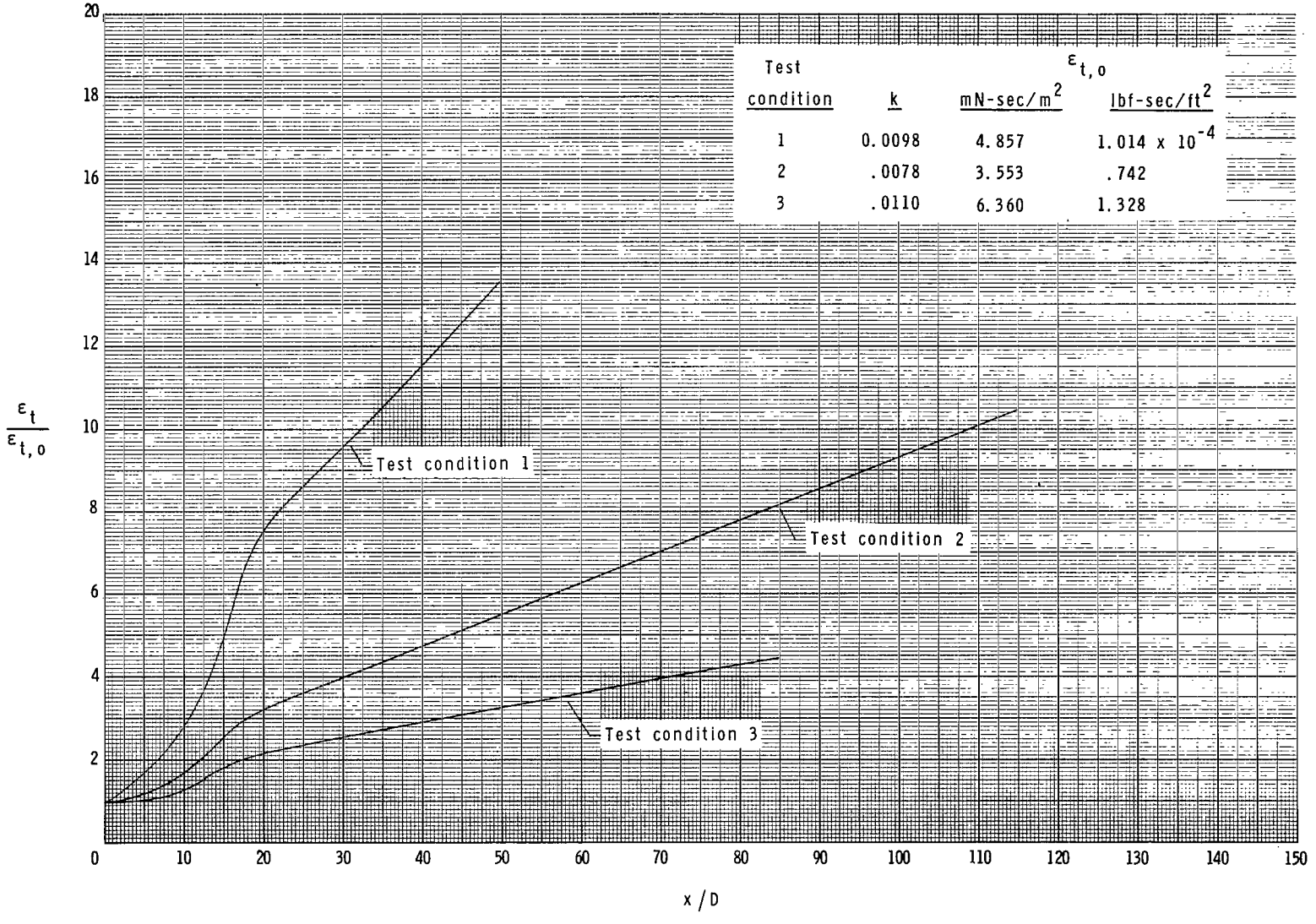

Figure 9.- Eddy viscosity distributions.

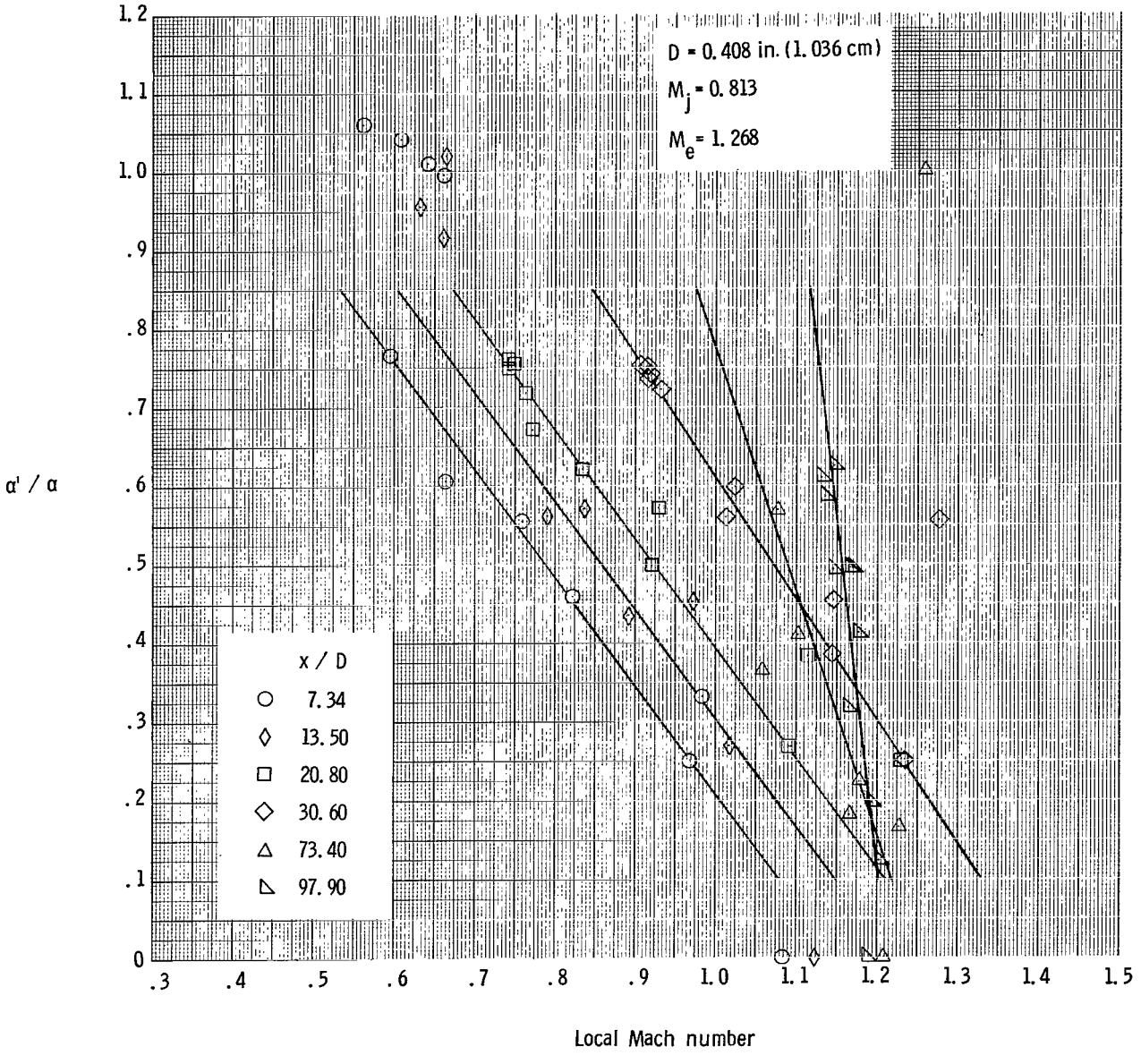

(a) Mass-concentration ratio as a function of local Mach number.

Figure 10.- Effect of gas sampling rates.

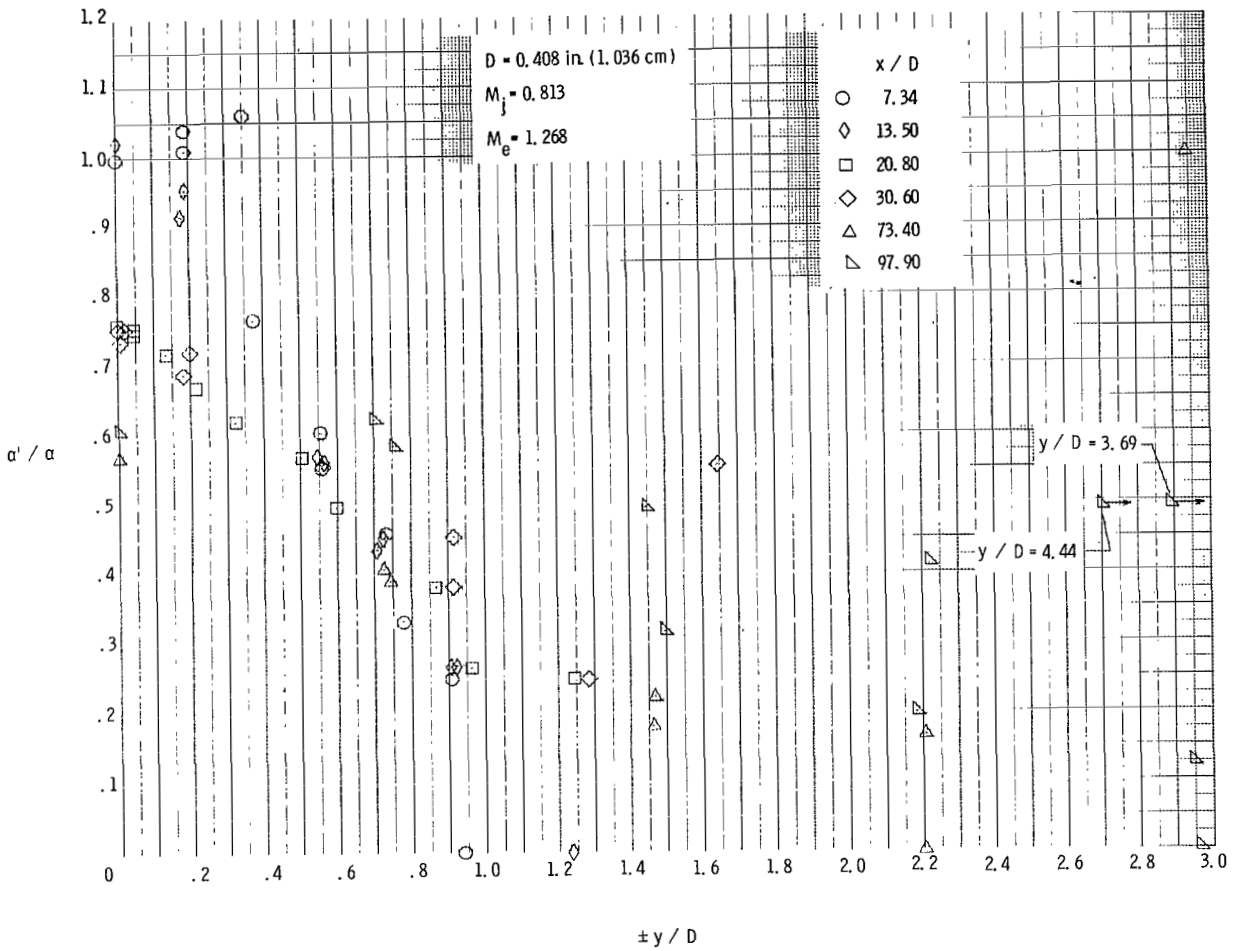

(b) Mass-concentration ratio as a function of nondimensional coordinate, y/D.

Figure 10.- Concluded.

05U 001 37 51 3US 69178 00903
AIR FORCE WEAPONS LABORATORY/AFWL/
KIRTLAND AIR FORCE BASE, NEW MEXICO 8711

ATT E. LOU BOWMAN, ACTING CHIEF TECH. LI

"The aeronautical and space activities of the United States shall be conducted so as to contribute . . . to the expansion of human knowledge of phenomena in the atmosphere and space. The Administration shall provide for the widest practicable and appropriate dissemination of information concerning its activities and the results thereof."

—NATIONAL AERONAUTICS AND SPACE ACT OF 1958

NASA SCIENTIFIC AND TECHNICAL PUBLICATIONS

TECHNICAL REPORTS: Scientific and technical information considered important, complete, and a lasting contribution to existing knowledge.

TECHNICAL NOTES: Information less broad in scope but nevertheless of importance as a contribution to existing knowledge.

TECHNICAL MEMORANDUMS: Information receiving limited distribution because of preliminary data, security classification, or other reasons.

CONTRACTOR REPORTS: Scientific and technical information generated under a NASA contract or grant and considered an important contribution to existing knowledge.

TECHNICAL TRANSLATIONS: Information published in a foreign language considered to merit NASA distribution in English.

SPECIAL PUBLICATIONS: Information derived from or of value to NASA activities. Publications include conference proceedings, monographs, data compilations, handbooks, sourcebooks, and special bibliographies.

TECHNOLOGY UTILIZATION PUBLICATIONS: Information on technology used by NASA that may be of particular interest in commercial and other non-aerospace applications. Publications include Tech Briefs, Technology Utilization Reports and Notes, and Technology Surveys.

Details on the availability of these publications may be obtained from:

SCIENTIFIC AND TECHNICAL INFORMATION DIVISION

NATIONAL AERONAUTICS AND SPACE ADMINISTRATION

Washington, D.C. 20546